

SYNTHESIS AND ELECTROCHEMICAL STUDIES OF FLUORENE AND BENZIMIDAZOLE
CONTAINING CONJUGATED POLYMERS

A THESIS SUBMITTED TO
THE GRADUATE SCHOOL OF NATURAL AND APPLIED SCIENCES
OF
MIDDLE EAST TECHNICAL UNIVERSITY

BY

İMGE NAMAL

IN PARTIAL FULFILLMENT OF THE REQUIREMENTS
FOR
THE DEGREE OF MASTER OF SCIENCE
IN
CHEMISTRY

JANUARY 2013

Approval of the thesis:

**SYNTHESIS AND ELECTROCHEMICAL STUDIES OF FLUORENE AND
BENZIMIDAZOLE CONTAINING CONJUGATED POLYMERS**

submitted by **İMGE NAMAL** in partial fulfillment of the requirements for the degree of **Master of Science in Chemistry Department, Middle East Technical University** by,

Prof. Dr. Canan Özgen
Dean, Graduate School of **Natural and Applied Sciences**

Prof. Dr. İlker Özkan
Head of Department, **Chemistry**

Prof. Dr. Levent Toppare
Supervisor, **Chemistry Dept., METU**

Assoc. Prof. Dr. Yasemin Arslan Udum
Co-Supervisor, **Advanced Technologies Dept., Gazi University**

Examining Committee Members:

Assoc. Prof. Dr. Metin Ak
Chemistry Dept., Pamukkale University

Prof. Dr. Levent Toppare
Chemistry Dept., METU

Assoc. Prof. Dr. Yasemin Arslan Udum
Advanced Technologies Dept., Gazi University

Assoc. Prof. Dr. Ali Çırpan
Chemistry Dept., METU

Assist. Prof. Dr. Emren Esentürk
Chemistry Dept., METU

Date: 18.01.2013

I hereby declare that all information in this document has been obtained and presented in accordance with academic rules and ethical conduct. I also declare that, as required by these rules and conduct, I have fully cited and referenced all material and results that are not original to this work.

Name, Last name: İMGE NAMAL

Signature :

ABSTRACT

SYNTHESIS AND ELECTROCHEMICAL STUDIES OF FLUORENE AND BENZIMIDAZOLE CONTAINING CONJUGATED POLYMERS

Namal, İmge
M. Sc., Department of Chemistry
Supervisor: Prof. Dr. Levent Toppare
Co-Supervisor: Assoc. Prof. Dr. Yasemin Arslan Udum

January 2013, 48 pages

The synthesis and characterization of two donor acceptor type conjugated polymers were investigated. The electrochemical properties were examined using cyclic voltammetry, spectroelectrochemistry and kinetic studies.

The increase in the alkyl chain length attached to the fluorene unit was investigated by the corresponding electrochemical characteristics. The synthesis was carried out via Stille coupling of 4,7-dibromo-4'-(tert-butyl)spiro[benzo[d]imidazole-2,1'-cyclohexane] and 2,5-bis(tributylstannyl)thiophene with 9,9-dihexyl-9H fluorene and 9,9-didodecyl-9H fluorene respectively. Both of the polymers were neutral state green polymers. They had optical band gaps of 2.46 and 2.54 eV respectively. Increasing the chain length resulted in an increase in solubility and processibility of the polymer but also an increase in the band gap. This was due to the increased bulkyness of the alkyl group, leading to a decrease in the effective conjugation and planarity. They both had distinctive π - π^* transitions, band structure and backbone that provides oxidative doping. P1, with the shorter alkyl chain had a lower oxidation potential than P2. Neither of the polymers was capable of being n-doped. They were both multichromic, revealing colors from neutral state green to doped state blue.

Keywords: Benzimidazole, Fluorene, increase of alkyl chain length, Electrochromism, Multichromic, Conjugated polymers, Donor Acceptor Theory

ÖZ

FLUOREN VE BENZİMİDAZOL İÇEREN KONJUGE POLİMERLERİN SENTEZİ VE ELEKTROKİMYASAL ÇALIŞMALARI

Namal, İmge
Yüksek Lisans, Kimya Bölümü
Tez Yöneticisi: Prof. Dr. Levent Toppare
Ortak Tez Yöneticisi: Doç. Dr. Yasemin Arslan Udum

Ocak 2013, 48 sayfa

İki donör akseptör tipi polymerin sentezi ve karakterizasyonu yapılmıştır. Polymerlerin elektrokimyasal özellikleri dönüşümlü voltametri, spektroeletrokimya ve kinetik çalışmaları sonucunda incelenmiştir.

Fluoren ünitesine bağlı alkil zincirindeki uzunluk artışının sonuçları elektrokimyasal özelliklerin değişimi izlenerek ölçülmüştür. Sentezde, 4,7-dibromo-4'-(tert-butil)spiro[benzo[d]imidazol-2,1'-sikloheksan] ve 2,5-bis(tributilstannil)tiyofen, 9,9-dihexzil-9H fluoren ve 9,9-didodesil-9H fluoren ile birleştirilmiştir. Polymerlerin her ikisi de nötral halde yeşildir. Optik bant aralıkları sırasıyla 2.46 ve 2.54 olarak bulunmuştur. Alkil zincir uzunluğundaki artış, çözünürlük ve işlenebilirlikte artışa neden olurken bant aralığını da arttırmıştır. Bunun nedeni alkil grubun sterik etkisinin artması ve efektif konjugasyon ve planerlikte azalmaya yol açmasıdır. İki polimer de belirgin $\pi-\pi^*$ geçişlerine, bant oluşumlarına ve oksidatif katkılanmaya uygun yapıya sahiptir. Alkil zinciri kısa olan polimer daha düşük oksitlenme potansiyeline sahiptir. İki polimer de negatif katkılanamamaktadır. Her iki polimer de multikromiktir ve yeşil ve mavi arası renkler gösterirler.

Anahtar kelimeler: Benzimidazol, Fluoren, Alkil Zincir Uzunluğu Artışı, Elektrokromizm, Multikromik, Konjüge Polymerler, Donör Akseptör Teorisi.

To my dearest family,

ACKNOWLEDGMENTS

First of all, I would like to express my sincere gratitude for my supervisor, Prof. Dr. Levent Toppare for being a role model with his patience, confidence and enthusiasm towards science and success. I am grateful to have his guidance help and support through my graduate studies.

I would like to thank my coadvisor Assoc. Prof. Dr. Yasemin Arslan Udum for her support and help during electrochromic studies.

I would like to thank Gönül Hızalan and Ali Can Özelçağlayan for their help and support during my thesis studies. I am grateful to have them as both labmates and friends.

I would like to thank Betül Eymur for her friendship, patience and care. I owe her a lot for her moral support in addition to the NMR measurements she has made for me.

I would like to thank Bengisu Çorakçı for being there for me when I needed. I am happy to find a friend that I get along with this well.

I would like to thank my lab mates for the enjoyable coffee breaks we spent.

I would like to thank my best friends for being a part of me and complementing my life. Even the ones that were living in most far were able to make me smile at most.

Lastly and mostly, I would like to express my dearest love and gratitude to my family. I would like to thank my mom for being a mentor and a support all through my life and being able to help me build my life and character without any judgments. I would like to thank my dad for having an endless understanding and for teaching me to keep my peace of mind in every situation. I would like to thank my brother for being my best friend, my buddy, my playmate and sometimes letting me be the younger one.

LIST OF TABLES

TABLES

Table 1.....37

LIST OF FIGURES

FIGURES

Fig. 1.1. (a) trans polyacetylene (b) cis polyacetylene	1
Fig. 1.2. Structures of some common conducting polymers	2
Fig. 1.3. Development of the band gap of polythiophene through increasing monomer units	4
Fig. 1.4. Band structures of metal, semiconductor and insulator	4
Fig. 1.5. Reversible doping of polythiophene	5
Fig. 1.6. Comparison of conductivities of metals, semiconductors and insulators	7
Fig. 1.7. Representation of solitons	8
Fig. 1.8. Polarons and bipolaron structures in poly(p-phenylenevinylene) and corresponding electronic representations	9
Fig. 1.9. Some examples of multichromic polymers with minor structural changes	11
Fig. 1.10. Stille, Suzuki and Yamamoto coupling reactions for synthesizing polythiophene	13
Fig. 1.11. Mechanism of Palladium catalyzed coupling reactions	14
Fig. 1.12. Resonance forms of polyisothianaphthene	15
Fig. 1.13. Band gap tailoring for conjugated polymers	16
Fig. 1.14. Benzimidazole	17
Fig. 2.1. Synthesis of 4,7-dibromobenzothiadiazole	20
Fig. 2.2. Synthesis of 3,6-dibromobenzene-1,2-diamine	20
Fig. 2.3. Synthesis of 4, 7-Dibromo-4'-(tert-butyl)spiro[benzo[d]imidazole-2,1'-cyclohexane]	21
Fig. 2.4. Synthesis of 2,5-Bis(tributylstannyl)thiophene	22
Fig. 2.5. Chemical Polymerization of P1	22
Fig. 2.6. Chemical Polymerization of P2	23
Fig. 2.7. Voltage change as a function of time	24
Fig. 2.8. Voltage change as a function of current	25
Fig. 2.9. Three electrode system	25
Fig. 3.1. Cyclic Voltammogram of P1 which was taken in a monomer free environment with a 0.1 M NaClO₄-LiClO₄/ACN solution.	28
Fig. 3.2. Scan rate dependence of P1 film in a 0.1 M NaClO₄-LiClO₄/ACN solution.	29
Fig. 3.3. Cyclic Voltammogram of P2 which was taken in a monomer free environment with a 0.1 M NaClO₄-LiClO₄/ACN solution.	30
Fig. 3.4. Scan rate dependence of P2 film in a 0.1 M NaClO₄-LiClO₄/ACN solution.	31
Fig. 3.5. Spectroelectrochemistry of P1 film on an ITO coated glass slide in monomer-free, 0.1 M NaClO₄-LiClO₄/ACN electrolyte–solvent couple at applied potentials (from 0 to 1.8V).	32
Fig. 3.6. L.a.b colors of P1 on an ITO coated glass slide in the neutral and oxidized states.	33
Fig. 3.7. Spectroelectrochemistry of P2 film on an ITO coated glass slide in monomer-free, 0.1 M NaClO₄-LiClO₄/ACN electrolyte–solvent couple at applied potentials (from 0 to 1.8V).	34
Fig. 3.8. L.a.b. colors of P2 film on an ITO coated glass slide in the neutral and oxidized states.	35
Fig. 3.9. Percent transmittance change and switching times for P1 monitored at 410 and 1310 nm in 0.1 M NaClO₄-LiClO₄/ACN electrolyte–solvent couple.	36
Fig. 3.10. Percent transmittance change and switching times for P2 monitored at 445 and 1320 nm in 0.1 M NaClO₄-LiClO₄/ACN electrolyte–solvent couple.	37
Fig. A.1. ¹H-NMR spectrum of 4,7-dibromobenzothiadiazole	43
Fig. A.2. ¹³C-NMR spectrum of 4,7-dibromobenzothiadiazole	44
Fig. A.3. ¹H-NMR spectrum of 3,6-dibromobenzene-1,2-diamine	44
Fig. A.4. ¹³C-NMR spectrum of 3,6-dibromobenzene-1,2-diamine	45
Fig. A.5. ¹H-NMR spectrum of 4, 7-dibromo-4'-(tert-butyl)spiro[benzo[d]imidazole-2,1'-cyclohexane]	45
Fig. A.6. ¹³C-NMR spectrum of 4, 7-dibromo-4'-(tert-butyl)spiro[benzo[d]imidazole-2,1'-cyclohexane]	46
Fig. A.7. ¹H-NMR spectrum of 2,5-bis(tributylstannyl)thiophene	46
Fig. A.8. ¹³C-NMR spectrum of 2,5-bis(tributylstannyl)thiophene	47

Fig. A.9. ^1H -NMR spectrum of P1
Fig. A. 10. ^1H -NMR spectrum of P2

47
48

LIST OF ABBREVIATIONS

ACN	Acetonitrile
BIm	Benzimidazole
BSe	Benzoselenadiazole
BTd	Benzothiadiazole
BTz	Benzotriazole
CB	Conduction Band
CHCl₃	Chloroform
CP	Conducting Polymer
CV	Cyclic Voltammetry
D-A	Donor Acceptor
D-A-D	Donor Acceptor Donor
DCM	Dichloromethane
ECD	Electrochromic Device
E_g	Band Gap Energy
HOMO	Highest Occupied Molecular Orbital
ITO	Indium Tin Oxide
OPV	Organic Photovoltaic Device
OLED	Organic Light Emitting Diode
LUMO	Lowest Unoccupied Molecular Orbital
NMR	Nuclear Magnetic Resonance
PA	Polyacetylene
THF	Tetrahydrofuran
VB	Valence Band

TABLE OF CONTENTS

ABSTRACT	v
ÖZ	vi
ACKNOWLEDGMENTS	ix
LIST OF TABLES	ix
LIST OF FIGURES	x
LIST OF ABBREVIATIONS	xii
CHAPTERS	1
1. INTRODUCTION	1
1.1. Conducting Polymers	1
1.2. Conduction Mechanism in Conducting Polymers	3
1.2.1. Band Theory	3
1.2.2. Doping	5
1.2.3. Solitons, Polarons, Bipolarons	7
1.2.4. Hopping	9
1.3. Applications of Conducting Polymers	10
1.3.1. Electrochromism	10
1.3.2. Advances in Electrochromic Conducting Polymers	12
1.4. Synthesis of Conducting Polymers	12
1.4.1. Chemical Polymerization	13
1.5. Tailoring the Band Gap of Conducting Polymers	15
1.5.1. Donor Acceptor Theory	17
1.5.1.1. Thiophene as the Donor Unit	17
1.5.1.2. Benzimidazole as the Acceptor Unit	17
1.5.1.3. Fluorene as the Donor Unit	18
1.6. Aim of Work	18
2. EXPERIMENTAL	19
2.1. Materials	19
2.2. Equipment	19
2.3. Synthesis	20
2.3.1. Synthesis of 4,7-dibromobenzothiadiazole	20
2.3.2. Synthesis of 3,6-dibromobenzene-1,2-diamine	20
2.3.3. Synthesis of 4, 7-Dibromo-4'-(tert butyl)spiro[benzo[d]imidazole 2,1'cyclohexane	21
2.3.4. Synthesis of 2,5-Bis(tributylstannyl)thiophene	22
2.3.5. Chemical Polymerization of P1	22
2.3.6. Chemical Polymerization of P2	23
2.4. Characterization of Conducting Polymers	23
2.4.1. Cyclic Voltammetry	23
2.4.2. Spectroelectrochemistry	26
2.4.3. Colorimetry	26
2.4.4. Kinetic Studies	26
3. RESULTS AND DISCUSSION	27
3.1. Electrochemical Characterization of Polymers	27
3.1.1. Cyclic Voltammogram of P1	27
3.1.2. Scan Rate Dependence of P1	28
3.1.3. Cyclic Voltammogram of P2	29
3.1.4. Scan Rate Dependence of P2	30
3.2. Spectroelectrochemistry Studies	31
3.2.1. Spectroelectrochemistry Studies for P1	31
3.2.2. Spectroelectrochemistry Studies for P2	33
3.3. Kinetic Studies	35
3.3.1. Kinetic Study of P1	35
3.3.2. Kinetic Study of P2	36
3.4. Summary of Results and Discussion	37

4. CONCLUSION	39
REFERENCES	40
APPENDIX	43

CHAPTER 1

INTRODUCTION

1.1. Conducting Polymers

30 years ago the only common properties of conventional polymers and metals were thought to be their processibility, strength, toughness and frictional resistance. Plastics replaced metals in many areas, but their lack of electrical conductivity limited their use in many electronic and optical devices. This aroused the necessity of producing superior materials that possess an electrical conductivity similar to metals but remain processible to a certain extent.

Although initial work for synthesizing conducting organic polymers was done by Letheby et al. in 1862 [1], the first steps of a major breakthrough was taken in Hideki Shirakawa's lab in 1977. The report of the date stated that polyacetylene, which was previously known as a black powder is made to mimic a metal in its appearance, as they increased the catalyst amount 1000 times by accident [2]. The subsequent contribution of Alan Heeger and Alan MacDiarmid to this work took it a step further. Shirakawa, Heeger and MacDiarmid proved that the conductivity of this very same polyacetylene film can be increased up to 12 orders of magnitude, obtaining a conductivity of 103 S/cm, upon oxidative doping with strong electron acceptors like iodine vapor [3]. In 2000, 23 years after the first experiment, Nobel Prize was awarded to these three scientists "for discovering and developing conductive polymers." [4]

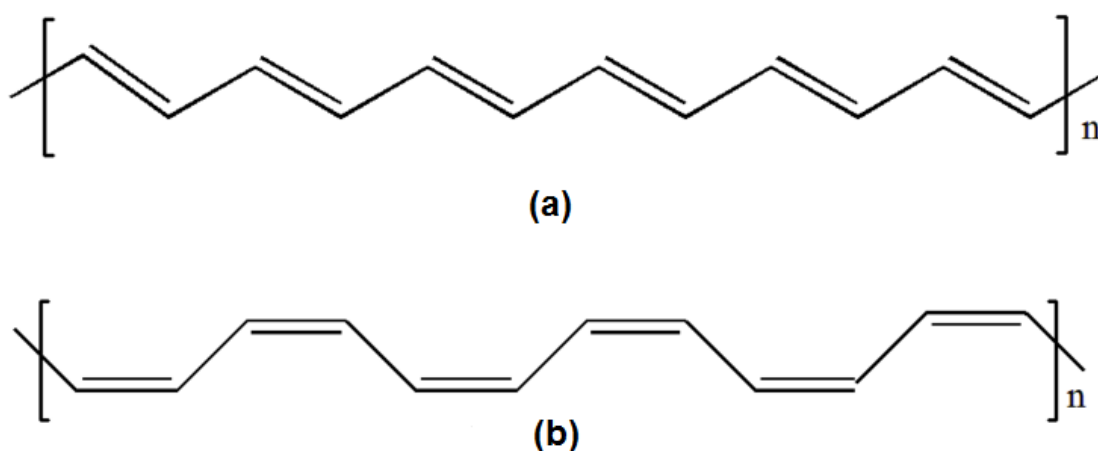


Fig. 1.1. (a) trans polyacetylene (b) cis polyacetylene

This research opened a new era both for academia and industry, providing an understanding of the chemistry, physics and materials science of conducting polymers. The oxidative coupling of the trans isomer of polyacetylene results with a thermodynamically stable polymer at room temperature (Figure 1.1(a)). Polyacetylene (PAC) possess the key characteristic of a conducting polymer; a conjugated π system with alternating single and double bonds all through the chain linked monomer units. Normally, it has localized electrons which disable the electrical conductivity. Upon doping, either by removing an electron through oxidation or adding an electron through reduction, it has a conductivity of a semiconductor.

Despite its very high (copper like) conductivity, doped PAC is very unstable, sensitive against humidity and oxygen, insoluble in many organic solvents and hard to process. All these limitations lead the scientists search for new PAC derivatives that are more stable and processible, retaining the high conductivity [5,6]. Unfortunately the conductivity of PAC cannot be obtained by these derivatives.

With the aim of obtaining conducting polymers better than PAC, new structures have been designed. Polythiophene [7], polypyrrole [8], polyfuran[9], poly(p-phenylene) [10] (PPP), poly(p-phenylenevinylene) [11] (PPV), polyfluorene, [12] polyaniline [13] (PAn) and polycarbazole [14] are some examples of new classes of conducting polymers (Figure 1.2). Especially heterocyclic polymers with an electron rich nature such as polypyrrole and polythiophene are very stable due to their low polymer oxidation potentials compared to PAC. They are also more processible, offering a wide range of derivatives, but none of these polymers exceeded the conductivity level of PAC.

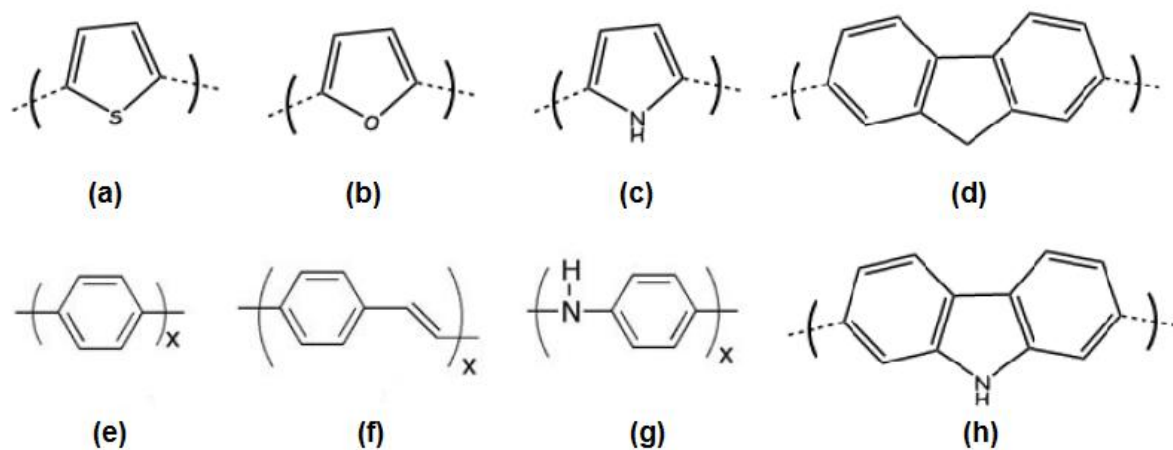


Fig. 1.2. Structures of some common conducting polymers. (a) polythiophene, (b) polyfuran, (c) polypyrrole, (d) polyfluorene, (e) poly(p-phenylene), (f) poly(p-phenylene vinylene), (g) polyaniline (h) polycarbazole

1.2. Conduction Mechanism in Conducting Polymers

The appeal of the research area of conducting polymers originates from the electronic properties of the polymer backbone, which arises from the extended conjugation. Charge carriers can move freely through the structure which leads to high conductivity. The movement of charge carriers (electrons and holes) along an electric field is called electronic conduction. Electronic conduction and thus conductivity increase is directly proportional with the increase of charge carriers. The electrical conductivity of a conductive polymer (σ) can be summoned by the equation;

$$\sigma = nq\mu$$

where n is the total number of charge carriers, q is the charge of the carriers and μ is the mobility of the charge carriers.

In order to visualize the concept, PAc is a suitable example with its simple structure. It is composed of sp^2 hybridized carbon atoms linked together with alternating single and double bonds through a chain, $(CH)_x$. Like most conducting polymers, its neutral state consists of very few charge carriers. A doping process has to be applied in order to increase the number of charge carriers (n) and cause a drastic increase in the conductivity.

Examining the equation, another important aspect influencing the conductivity of the polymer is the charge carrier mobility (μ). The charge mobility is about how easily the charge moves. This movement can be along the polymer chain (intra-chain movement), from one polymer chain to another (inter-chain hopping) and also from particle to particle (inter particle mobility). Intra chain movement is dependent on effective conjugation of the chain, where inter chain hopping is about the stacking of the polymer.

For providing a deeper understanding for the conductivity of conducting polymers, concepts like band theory, doping process, soliton, polaron-bipolaron and hopping should be explained.

1.2.1. Band Theory

Introducing the doping process, addition or removal of electrons in conjugated polymers, band theory must be discussed first. It is a theory mostly used to explain the conductivity of metals, semiconductors and insulators. As conducting polymers have conductivity as much as a semiconductor, their electronic behavior can also be explained by this theory.

When two p orbitals combine to form a π bond, 2 molecular π orbitals are formed; one bonding and one anti-bonding. There is a certain energy difference between the bonding and anti-bonding orbitals. Increasing the conjugation, number of both bonding and anti-bonding orbitals increases, causing formation of two discrete energy bands; valence band (highest occupied molecular orbital) and conduction band (lowest unoccupied molecular orbital). The energy difference between these two bands is called band gap (E_g). It is equal to the energy needed for a π - π^* transition of the neutral conjugated polymer (Figure 1.3).

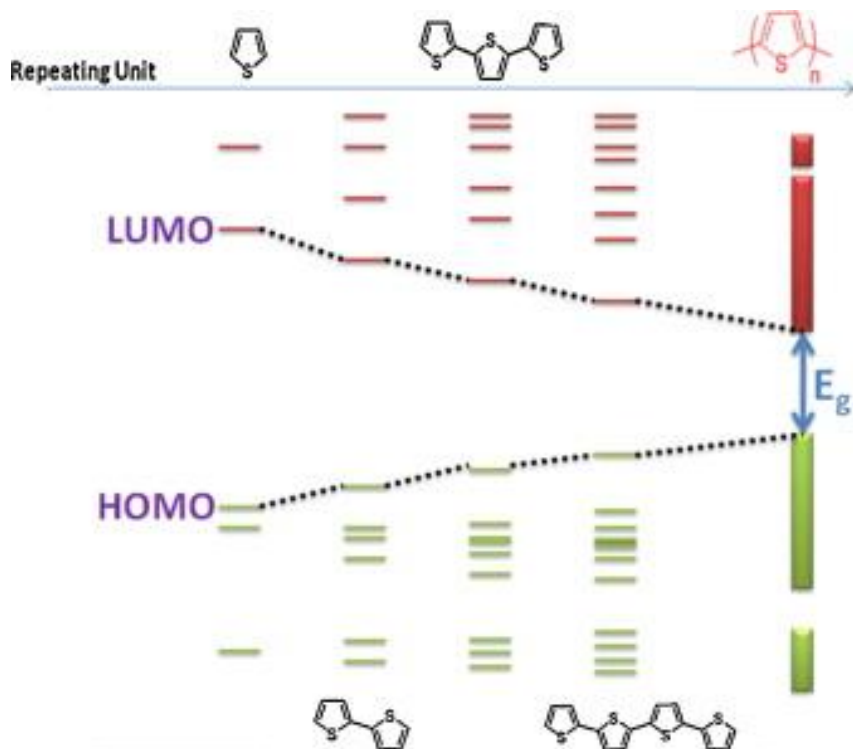


Fig. 1.3. Development of the band gap of polythiophene through increasing monomer units [15].

The width of the band gap determines whether the material is a metal, semiconductor or an insulator. Metals have no band gap, enabling the continuous flow of electron through the material. Insulators, on the other hand have a very large band gap that disables the transport of the electron from the valence band to the conduction band. Semiconductors have relatively smaller band gaps compared to insulators and they can be doped to increase the conductivity (Figure 1.4). The band gaps of semiconductors usually differ in the range of 1-4 eV which correlates to the visible spectrum, displaying intense color.

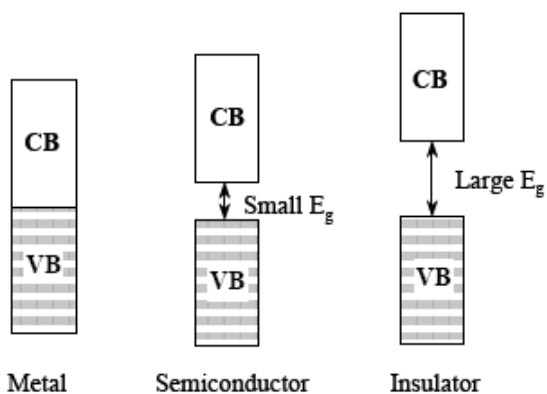


Fig. 1.4. Band structures of metal, semiconductor and insulator.

1.2.2. Doping

Doping can be defined as increasing the conductivity of the material with the addition of an 'impurity'. This process in conducting polymers, changes the oxidation state of the material, keeping the structure intact, by either inserting or removing an electron from the π conjugated system [16, 18]. The addition of an electron to the conduction band (reduction) is called n-doping, where the removal of an electron from the valance band (oxidation) is called p-doping. (Figure 1.5)

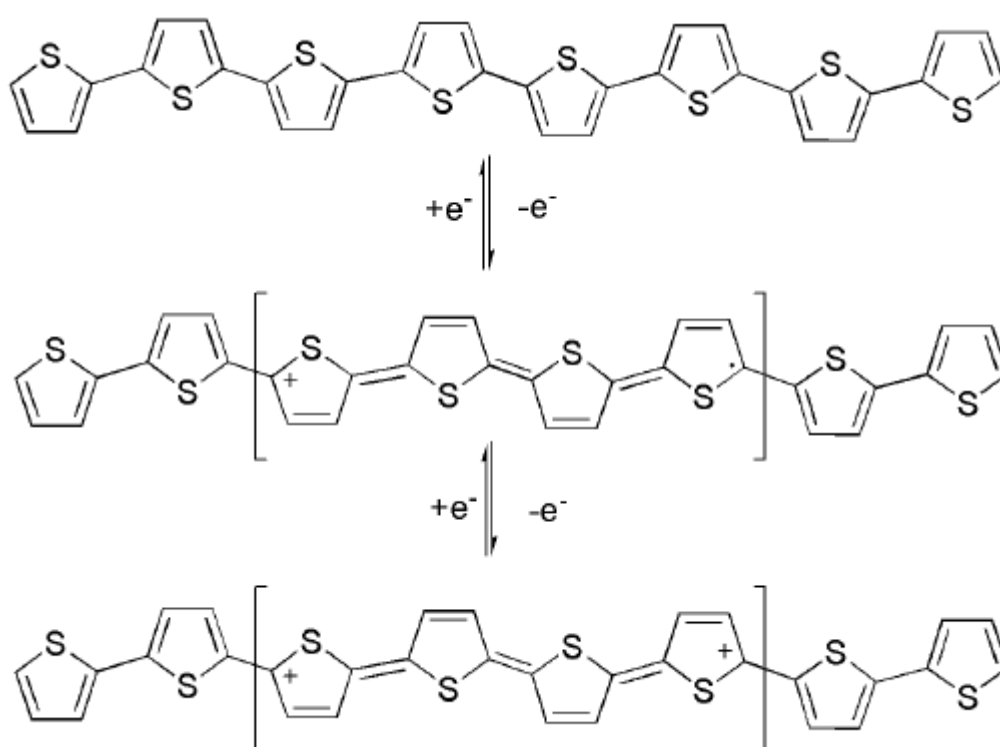
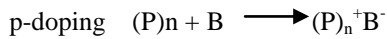


Fig. 1.5. Reversible doping of polythiophene

Doping can be accomplished by variety of methods. Some of them are; chemical, photochemical, electrochemical and interfacial doping. In order to maintain the overall neutrality, the charged polymer is neutralized with a counter ion in each of these methods.

In chemical doping, doping process is carried out using a strong oxidizing or reducing agent. The reactions are as following;

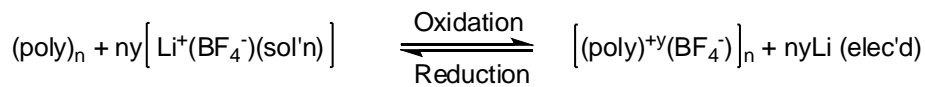




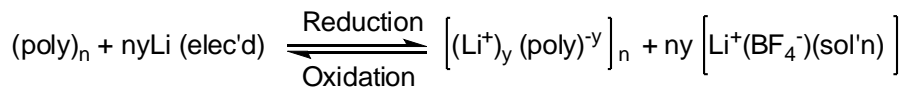
Here, A^+ and B^- are the dopant ions. The dopants can be gaseous like AsF_3 , AsF_5 , PF_3 or I_2 or oxidizing agents in solution like $FeCl_3$. The doping level, therefore the conductivity can be adjusted by the vapor pressure or concentration of the dopant, temperature of the medium and structure of the polymer [19].

Electrochemical doping is a more common way of doping. The frequency of its usage lies in the better control of doping level. The oxidation or reduction proceeds with the given voltage, enabling reproducible and controllable experimentation. The counter ion in the electrolyte diffuses in and out of the polymer to provide charge neutralization. The reactions are as follows;

For p-type;



For n-type;



By doping, the conductivity of the polymer is raised from $10^{-10} - 10^{-5} \text{ S cm}^{-1}$ (undoped) to $\sim 1-10^4 \text{ S cm}^{-1}$ (fully doped). This process enables the tuning of the conductivity of polymer from insulator to metal range. Figure 1.6 shows the conductivity ranges of polyacetylene polypyrrole and polythiophene.

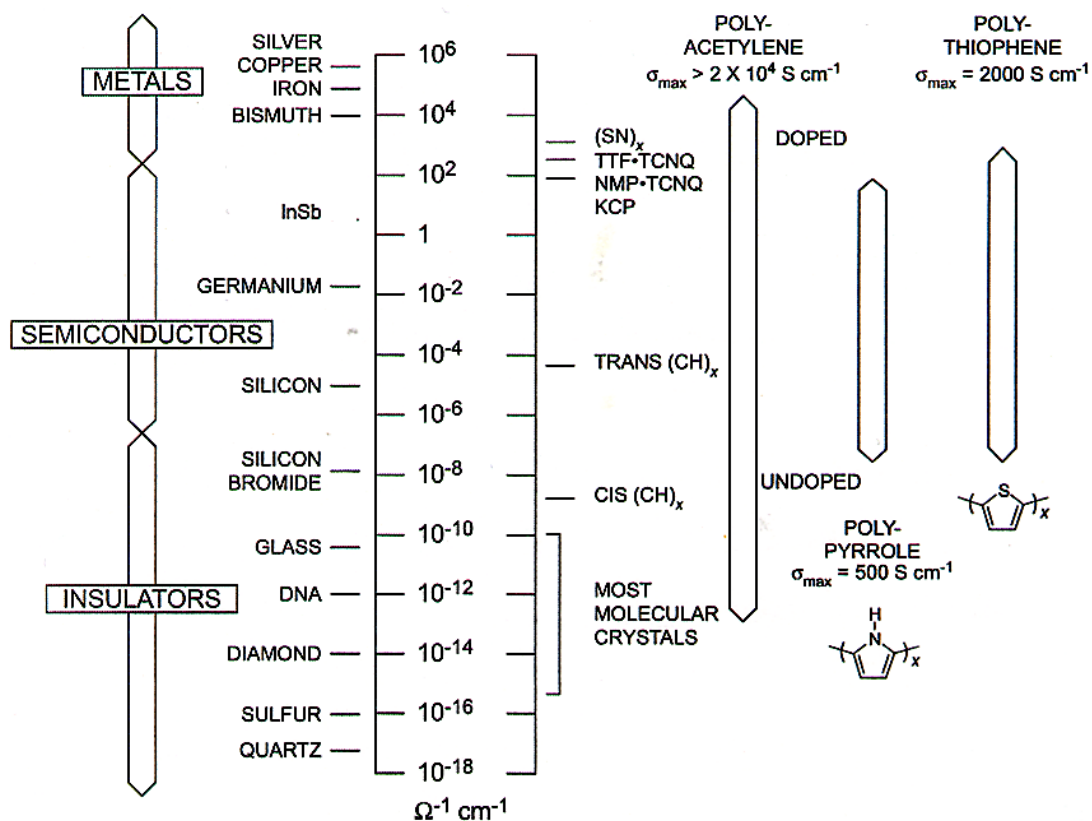


Fig. 1.6. Comparison of conductivities of metals, semiconductors and insulators.

As a result of doping process, some deformations called solitons, polarons and bipolarons are produced on the polymer. These deformations cause the formation of new energy levels, enabling easier movement for the electrons [20, 21].

1.2.3. Solitons, Polarons, Bipolarons

Doping causes formation of solitons, polarons and bipolarons. They are conjugational defects on the polymer chain.

If the conjugated polymer has two degenerate (energetically equivalent) ground state structures, like in the case of polyacetylene, solitons are likely to be produced upon doping. There are three types of solitons; neutral, positive and negative solitons. Neutral solitons are formed at the interface of the two degenerate structures on the same polymer chain. It does not have charge. There is an energy level that has a single electron occupied, causing the spin to be $\frac{1}{2}$. Upon electrochemical oxidation (p-type doping), an electron is removed and a positive soliton is produced. By reduction (n-type doping) an electron is inserted and a negative soliton is generated. (Figure 1.7)

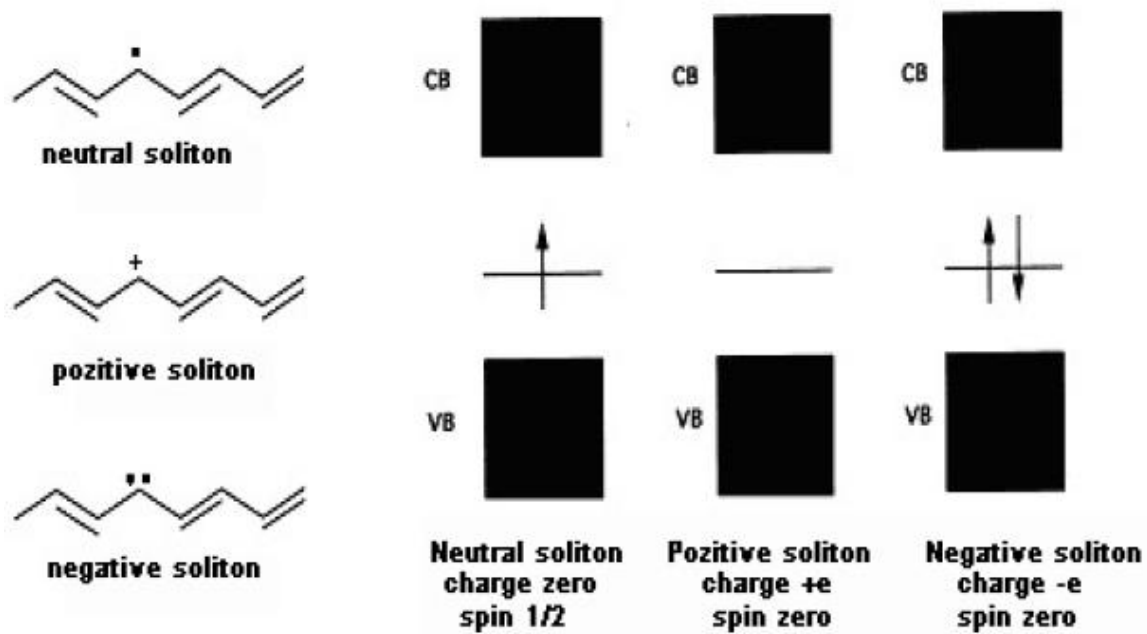


Fig. 1.7. Representation of solitons

For conjugated polymers that have non-degenerate ground states like PPV, removal of one electron breaks a double bond on the conjugated structure, leaving a radical and a cation. This is called a polaron. Further oxidation causes formation of dication on the chain, called bipolarons (Figure 1.8). The formation of bipolarons instead of increase of polarons on the chain is thermodynamically favored.

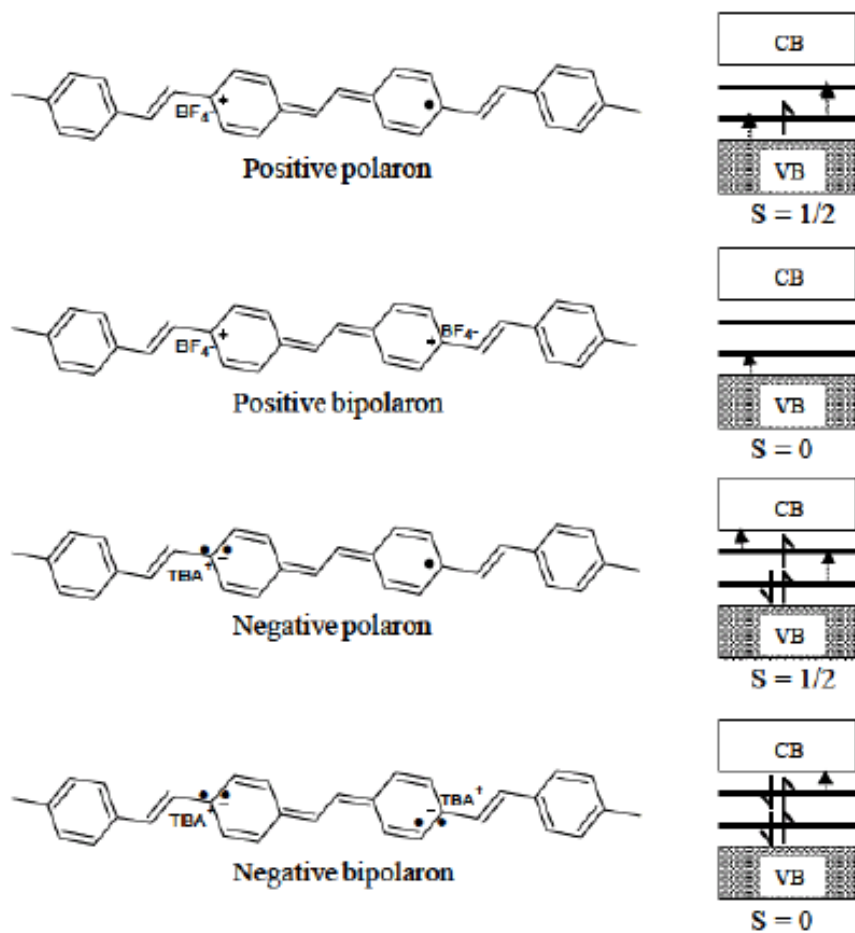


Fig. 1.8. Polarons and bipolaron structures in poly(p-phenylenevinylene) and corresponding electronic representations.

1.2.4. Hopping

In order to understand the conduction process in conjugated polymers, there is another important mechanism other than doping; hopping mechanism. The electron movement is not restricted along the polymer chain. It can be transported from one chain to another or from one segment of the polymer to another. The hopping movement is classified according to the range of the motion. The hopping conduction can be accomplished either by hopping to nearest neighbor or to a longer range. The efficiency of nearest neighbor hopping depends on effective conjugation along the chain, where hopping to a longer range, to another chain depends on the orientation of the polymer chains.

1.3. Applications of Conducting Polymers

Conducting polymers have novel properties, which encourages their usage in several application areas. The applications can be divided mainly into two groups; applications that use conducting polymers because of their conductivity and applications that use conducting polymers due to their electroactivity.

In applications that utilize the conductivity of the polymer, the advantages of using conducting polymers are their light weight, increased biocompatibility, ease of manufacture and relatively low cost compared to metals and other semiconductors. They are used as electrostatic materials, conducting adhesives, electromagnetic shielding materials, printed circuit boards, artificial nerves, antistatic clothing, piezoceramics, aircraft structures and active layers of diodes and transistors.

The second group of applications utilizes the electroactivity of the polymer. Some of these application areas are in; electrical displays, chemical biochemical and thermal sensors, rechargeable batteries, solid electrolytes, drug release systems, optical computers, ion exchange membranes, electromechanical actuators, smart structures, switches and electrochromic devices. Nearly all of these applications have emerged from the research area of molecular electronics and the advantage of structural modification ability in conducting polymers makes them good candidates for further application areas.

One of the main research areas that conjugated polymers are involved is electrochromic devices. They are mostly preferred over inorganic electrochromic materials due to their higher processibility and high degree of color tailorability. The use of conducting polymers as potential electrochromic device materials is also investigated in this work.

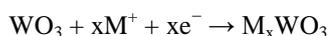
1.3.1. Electrochromism

Electrochromism can be defined as the reversible change in the observed reflectance or transmittance of the polymer due to the proceeding electrochemically induced oxidation-reduction reaction. The change is mostly observed on the color of the polymer. The color change of the polymer upon applied potential should be persistent. It either happens from transparent state to colored state or from one colored state to another. The reason of the color change or coloration is the new absorption bands produced by the electron transfer during the electrochemical reaction. A reverse transfer of the electron bleaches the polymer. If the polymer has many colors, it is named as polyelectrochromic and the process is called multicolor electrochromism [22]. Electrochromic materials find application in optical displays, smart windows, rearview mirrors, etc.

Electrochromic materials should be qualified in certain categories. These categories can be listed as; electrochromic memory, optical contrast, switching speed, coloration efficiency and stability. Electrochromic memory is the ability of the material to remain in its colorized state without applying further potential. The optical contrast is the transmittance difference between two different colored states seen in visible region. Coloration efficiency is the change in optical density per unit charge given. Finally, stability is the ability of the polymer to retain its electrochromic properties for a large number of switching cycles.

There are three types of electrochromic materials; transition metal oxides, organic small molecules and conductive polymers.

Transition metal oxides are the most studied electrochromic materials in the past 30 years [23]. Especially tungsten oxide, WO_3 , have been frequently used. The corresponding reaction of WO_3 is;



with $\text{M}^+ = \text{H}^+, \text{Li}^+, \text{Na}^+, \text{or } \text{K}^+$ [24].

Here WO_3 is transparent where M_xWO_3 is in blue color. The reduction of WO_3 , which is a material suitable for cathodic ion insertion, causes the blue color. The coloration can be reversed by an electrochemical oxidation reaction.

For the second class of electrochromic materials, organic small molecules, the most popular example are bipyridiliums. Also known as viologens, they show intense color upon reduction from transparent dicationic state to radicalic cations [25].

Conducting polymers are the most popular electrochromic materials due to their relatively easier and cheaper production, enhanced mechanical properties, short response time, high optical contrast, high coloration efficiency, better UV stability, independence of angle of vision and ability to control electronic properties over structural modifications. Tuning the electronic character of the neutral polymer, π - π^* transition can be adjusted through the electromagnetic spectrum [26]. These advantages grounded the use of conjugated polymers in smart windows, optical shutters and rearview mirrors. Examples of multichromic conducting polymers are shown in Figure 1.9.

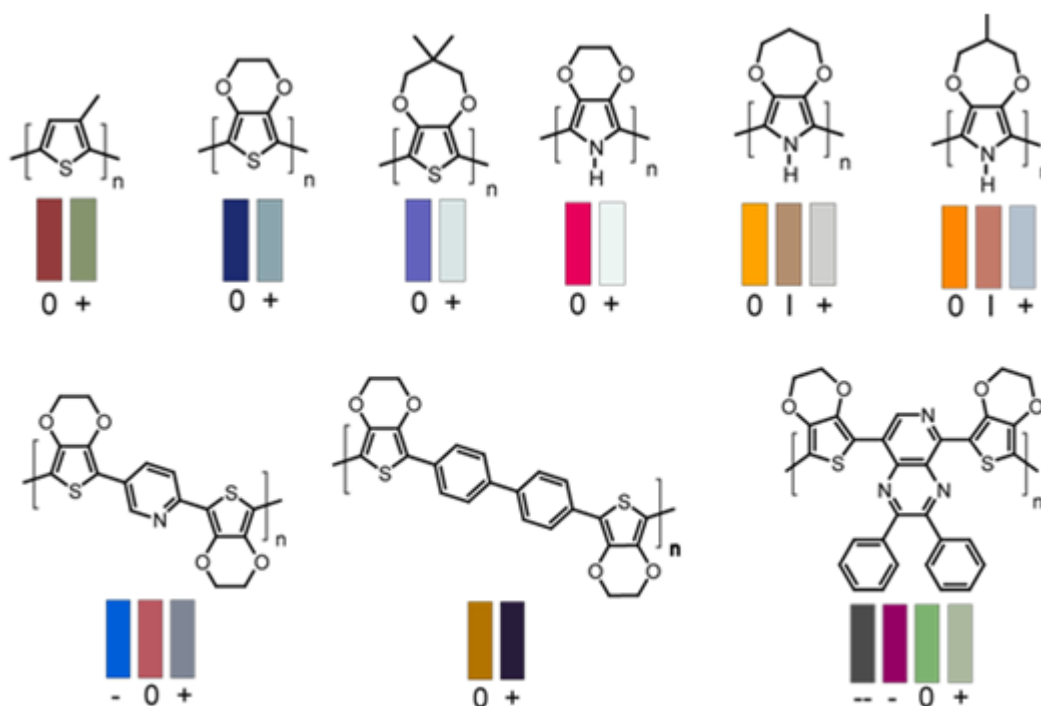


Fig. 1.9. Some examples of multichromic polymers with minor structural changes

The mostly used conjugated polymers have been polypyrrole (PPy), polythiophene (PTh), polyethylenedioxythiophene (PEDOT) and polyaniline (PANI). They are used in thin film form. The oxidation and reduction reactions causing a reversible insertion and removal of ions through the film, changes the π electronic character of the film.

A conducting polymer has a band gap (E_g) in its neutral state and therefore it displays a π - π^* transition. The band gap is measured by drawing a tangent to the onset of the π - π^* absorption peak. Upon oxidation, a new absorption band appears in the near IR region corresponding to the polarons produced along the chain. Further oxidation causes the intensity of the neutral absorption and polaron bands to decrease, generating a bipolaron band. All these causes change in color and transmittance of the polymer [27].

1.3.1.1. Advances in Electrochromic Conducting Polymers

In search of novel electrochromic conducting polymers, the properties that the scientists have been looking for are fast switching times, high contrast ratio, variable colors upon easy structural modifications and stable oxidized states.

The first conducting polymer that was reported as an electrochromic material was polyaniline (PANI). Goppelströderer et al. reported the use of PANI as an active layer of electrochromic materials in 1876 [28]. Later; the electrochromism of polypyrrole was studied by Diaz et al. In 1979 [29]. Reduced polypyrrole has a pale yellow color, which turns into dark blue upon oxidation. The only drawback for using polypyrrole was its tendency to degrade upon successive switching.

Among all, polythiophene and its derivatives have grabbed the greatest attention owing to the variety of colors upon small structural changes and the relatively higher processibility [30]. Polythiophene films have red color ($\lambda_{max}=490$ nm) which changes into blue ($\lambda_{max}\approx 800$ nm) upon oxidation.

Today, suitable candidates for electrochromic conducting polymers that have overcome the problem of solubility are being used for commercial applications of electrochromic devices. These valuable structural designs should also be used for other photovoltaic device applications.

1.4. Synthesis of Conducting Polymers

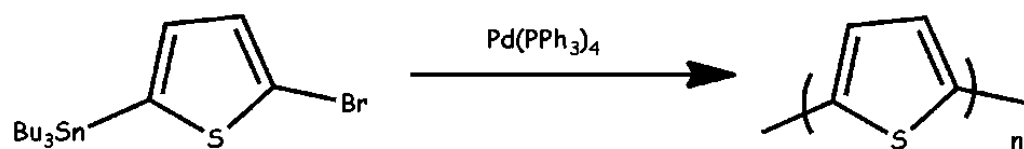
There are several ways to synthesize conducting polymers. Some of these methods are; chemical polymerization, electrochemical polymerization, photochemical polymerization, solid state polymerization, emulsion polymerization, plasma polymerization, graft polymerization, pyrolysis, etc [31]. The most commonly used methods of all are chemical and electrochemical polymerization.

The chemical polymerization processes result with a neutral polymer. Further doping is needed to obtain conductivity. Electrochemical polymerization, on the other hand produces already doped polymers. Chemical polymerization is more time consuming than electrochemical polymerization. Also thickness control is easier in electrochemical polymerization. But the neutral polymer produced by chemical polymerization is more stable and available for long term usage.

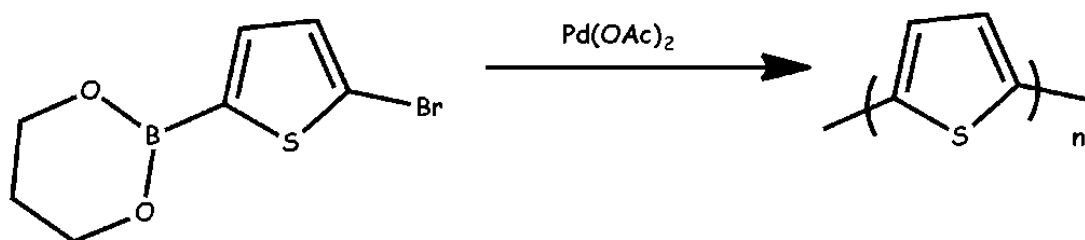
1.4.1. Chemical Polymerization

Chemical polymerization is the most suitable method for producing large amounts of neutral polymer [32, 33]. Chemical polymerization is carried out either by oxidation of monomer by transition metal halides or by metal catalyzed cross coupling reactions. Some of the most popular coupling reactions are shown in Figure 1.10 [34]. The oxidants create active cation radicals from monomers, while this process continues; the already produced cation radicals also react with monomers producing oligomers and polymers respectively. The synthesized polymer is not soluble in the reaction solvent so it precipitates, enabling an easy separation.

STILLE



SUZUKI



YAMAMOTO

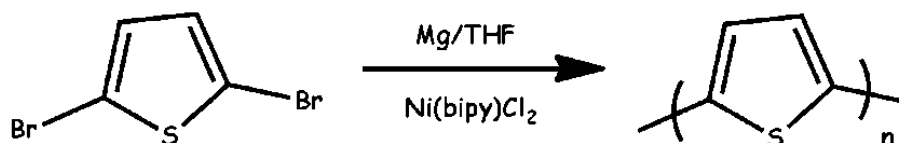


Fig. 1.10. Stille, Suzuki and Yamamoto coupling reactions for synthesizing polythiophene

The metals used in chemical polymerization reactions are generally palladium, nickel or iron. Palladium catalyzed cross coupling reactions have the following mechanism; the palladium is reduced from $\text{Pd}(\text{II})$ to $\text{Pd}(0)$, producing an active complex [35]. The halide is added to the $\text{Pd}(0)$ - ligand complex. This causes oxidation of $\text{Pd}(0)$ to $\text{Pd}(\text{II})$ species. Then nucleophile is transferred to this

oxidized Pd(II) ligand complex eliminating the halide. The Pd(II) linked to two ligands undergoes reductive elimination to yield the product and it reduces back to Pd(0) state (Figure 1.11)

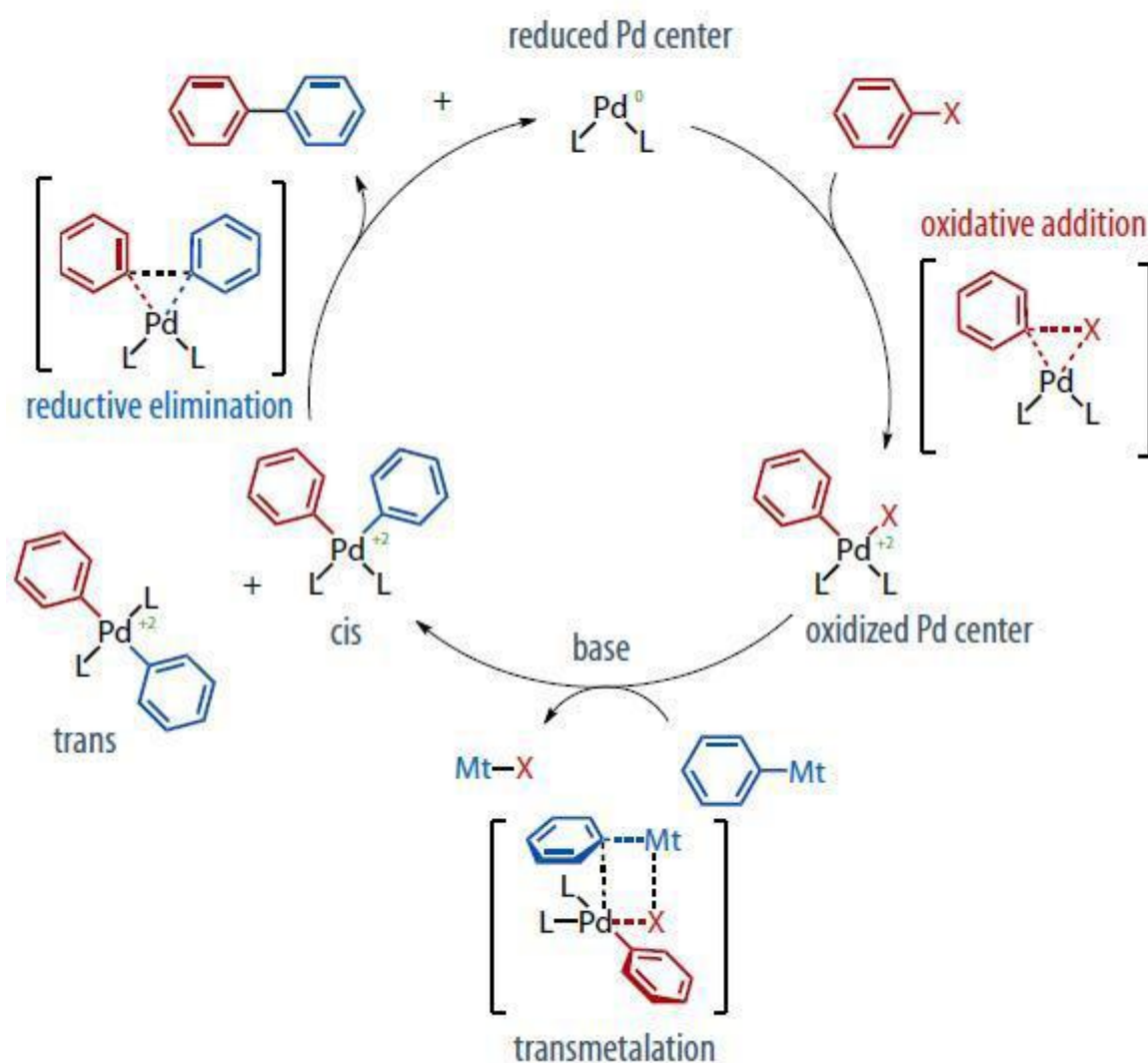


Fig. 1.11. Mechanism of Palladium catalyzed coupling reactions.

The name of the palladium catalyzed reaction changes with changing organometallic reagent. When Sn is used as a reagent, the cross coupling reaction is called Stille Coupling. Stille Coupling is used to synthesize the conducting polymer involved in this work. The method is used for coupling organostannanes and substituted halides. It is advantageous to use Stille Coupling reactions as it is applicable for a wide range of molecules. It is fast, and not very sensitive to air. The only drawback of Stille Coupling is that tin groups are highly toxic and must be handled with care [36].

1.5. Tailoring the Band Gap of Conducting Polymers

The prerequisite for a finite band gap is being composed of alternating single and double bonds in a conjugated system. It is assumed that all the conjugated C-C bonds have the same bond length with a complete delocalization leading to a graphite-like conduction. In reality, the delocalization is not as homogenous as it is assumed. Phenomena like electron-phonon coupling and electron-electron correlation cause the localization of π electrons, leading to an increase in the band gap in polyenic systems [37]. In the light of this knowledge, energy of bond length alternation (E_{BLA}) can be counted as having the greatest effect in controlling the band gap (E_g). Structural modifications for obtaining a reduced bond length alternation decrease the band gap [38].

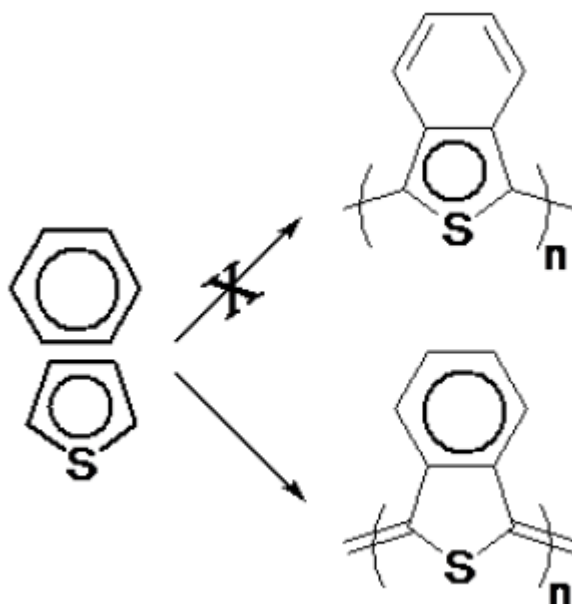


Fig. 1.12. Resonance forms of polyisothianaphthene

As it was stated before, aromatic conducting polymers, unlike polyenic conducting polymers, have non-degenerate ground states in their neutral form. Thus they have two different structures which are energetically unequal. The aromatic form is energetically more stable but the quinoid form has a higher energy and lower band gap [39]. The aromatic form needs to have aromatic stabilization resonance energy in order to transform into the quinoid form. This resonance energy (E_{res}) constrains the aromatic π electrons within the ring, preventing the delocalization through the chain. An example for this effect can be polyisothianaphthene (PITN). PITN energetically favors to be in quinoidal state rather than aromatic state because benzene with aromatization energy of 1.56 eV is more aromatic than thiophene (1.26 eV) (Figure 1.12). The resulting band gap of PITN is 1.1 eV which is lower than polythiophene [40]. Fused systems like PITN are frequently used in order to lower the band gap. One major disadvantage of these fused systems is their low stability.

Another factor that affects the band gap of aromatic conducting polymers is the rotation around the single bonds on the structure. As the rotation forms an angle θ between respective units, the planarity is disrupted and the π electron delocalization through the conjugated chain is limited. This causes an increase in the band gap in an amount of E_θ . As a consequence, regioregular poly(3-alkylthiophene)s show lower band gaps than polythiophenes with flexible side chains.

The most unobvious way of tailoring the band gap of conjugated polymers is to introduce electron donating or electron withdrawing substituents to the main chain. Inductive and mesomeric effects of the substituents (E_{sub}) affect the HOMO-LUMO values to a considerable extent. The inclusion of electron donating or withdrawing substituents to the main chain is used to increase the energy of the HOMO electrons, and decrease the energy of the LUMO electrons respectively. Therefore the band gap decreases.

The fifth factor affecting the band gap is the interaction between the molecules. The intermolecular interactions (E_{int}) can have a great impact on band gap in some cases.

As a result, the dependence of the band gap of a conducting polymer to the five factors stated above can be summed by the equation:

$$E_g = E_{\text{BLA}} + E_{\text{res}} + E_{\text{sub}} + E_\theta + E_{\text{int}} \quad [3].$$

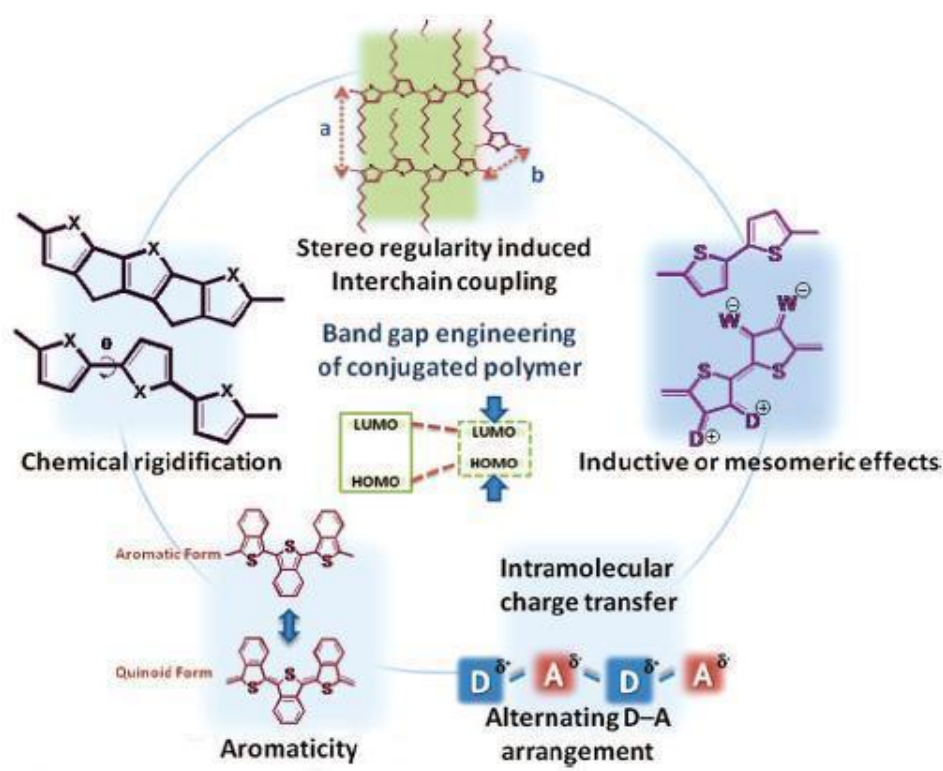


Fig. 1.13. Band gap tailoring for conjugated polymers.

1.5.1. Donor Acceptor Theory

The donor acceptor theory is a cornerstone for band gap engineering of conducting polymers. It is embraced as one of the most efficient ways to tune the band gap as it offers a wide range of possibilities for synthesis. This concept is first introduced in 1992 by Havinga et al [41].

The alternating donor and acceptor units in a polymer cause broadening in valence and conduction bands. The double bond character between the donor and acceptor is very strong because of the strong resonance energy between the compartments [42]. This energy between electron rich donor and electron deficient acceptor moieties causes hybridization between the HOMO of the donor and the LUMO of the acceptor. This also causes reduction in the bond length alternation giving rise to a decrease in the band gap [43].

1.5.1.1. Thiophene as the Donor Unit

Thiophene and its derivatives have been widely used as donor units according to their electron rich nature. Increasing the highest occupied molecular orbital by this electron rich nature lowers the band gap. π conjugated materials with low band gaps are designed.

1.5.1.2. Benzimidazole as the Acceptor Unit

Benzimidazole is composed of two fused cyclic compounds; imidazole and benzene (Fig. 1.14). It is one of the benzazole derivatives. Other benzazole derivatives used for synthesis of electrochromic materials are; benzothiadiazole, benzotriazole and benzoselenadiazole.

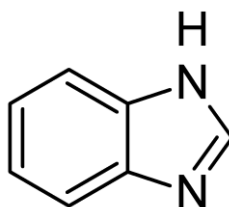


Fig. 1.14. Benzimidazole

Benzazole derivatives are widely used as acceptor units. They have high coloration efficiency, high electron transport ability, fast switching times and high optical contrast. The homopolymer of benzimidazole has high thermal stability and broad absorption. The conjugated structure enables its conductivity upon doping. Due to these properties, benzimidazole can be introduced into the structure for electrochromic and solar cell applications [44]. The use of benzimidazole in the polymer structure as an acceptor is not as widely studied as other benzazole derivatives. Also the pendant group that is attached is not a commonly used one. Due to these reasons, a benzimidazole derivative is introduced into the structure as an acceptor in this study.

1.5.1.3. Fluorene as the Donor Unit

Polyfluorenes are polymers with high hole mobility. Their electron mobility is low which can be improved by introducing fused structures such as benzimidazole into the structure. High quantum efficiencies are obtained by solar cell applications of fluorene containing conjugated polymers but problems like the poor solubility and low processibility leads to introduction of alkyl chains. It is reported that physical properties are affected by altering the length of the side chains but the relationship still remains poorly understood. Therefore introduction of different alkyl chains into the fluorene structure is investigated in this study.

1.6. Aim of Work

The aim of this study is to synthesize and investigate the electronic properties of benzimidazole, fluorene and thiophene containing polymers. The random copolymerization of 4,7-dibromo-4'-(tert-butyl)spiro[benzo[d]imidazole-2,1' cyclohexane] and 2,5-bis(tributylstannyl)thiophene is done with 9,9-dihexyl-9H fluorene and 9,9-didodecyl-9H fluorene respectively via Stille Coupling. The study is focused on investigating the effects of introducing different alkyl chains on the fluorene structure. Also effects of benzimidazole moiety with a rarely used pendant group are discussed. The characterization of the polymers are planned to be done with cyclic voltammetry, spectroelectrochemistry and kinetic studies and the electronic properties of the polymer will be investigated.

CHAPTER 2

EXPERIMENTAL

2.1. Materials

All chemicals were purchased from commercial sources and used without further purification except tetrahydrofuran (THF). THF was distilled over benzophenone and Na prior to use. 4-(Tert-butyl)cyclohexanone, 9,9-dihexyl-9H fluorene and 9,9-didodecyl-9H fluorene were obtained from Sigma Aldrich. 4,7-Dibromobenzothiadiazole [45], 3,6-dibromobenzene-1,2-diamine [46] and 2,5-bis(tributylstannyl)thiophene [47] were synthesized according to the reports published previously. The reactions are carried out under argon atmosphere unless stated otherwise. The following chemicals are used throughout the reactions; 2,1,3-Benzothiadiazole (Aldrich), hydrobromic acid (HBr, 47%) (Merck), bromine (Br₂) (Merck), 2,5-dibromothiophene (Aldrich), sodium borohydride (NaBH₄) (Merck), chloroform (CHCl₃) (Aldrich), toluene (Aldrich), hexane (C₆H₁₄) (Aldrich), dichloromethane (DCM) (Aldrich), ethylacetate (EtOAc) (Aldrich), tributyltin chloride (Sn(Bu)₃Cl, 96%) (Aldrich), n-butyllithium (n-BuLi, 2.5M in hexane) (Acros Organics), manganese dioxide (MnO₂) (Aldrich).

2.2. Equipment

Electrochemical studies were performed using a PST050 Voltalab potentiostat. A three-electrode cell was utilized where an ITO coated glass slide was used as the working electrode. A platinum wire and a Ag wire were used as the counter and pseudo reference electrodes. The measurements were carried out at room temperature under nitrogen atmosphere. The value of NHE is taken as -4.75 eV vs vacuum to calculate the HOMO and LUMO levels.

A Varian Cary 500 Spectrophotometer was used to record the UV/Vis/nIR spectra with a scan rate of 2000 nm/min. The potentiostat/galvanostat used for the spectroelectrochemical studies was a Solartron 1285. A Minolta CS-100A Chroma Meter with a 0/0 (normal/normal) viewing geometry was used in order to accomplish colorimetric measurements.

¹H NMR and ¹³C NMR spectra were taken on a Bruker Spectrospin Avance DPX-400 Spectrometer. CDCl₃ was the solvent and the chemical shifts were recorded relative to the internal standard; tetramethylsilane (TMS).

2.3. Synthesis

2.3.1. Synthesis of 4,7-Dibromobenzothiadiazole (1)

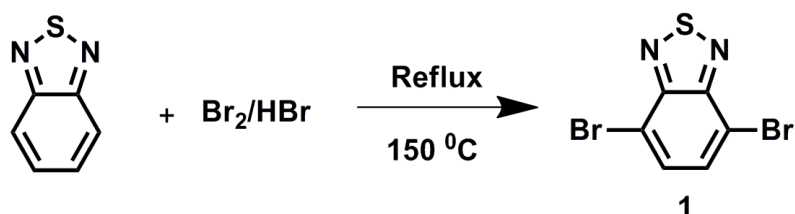


Fig. 2.1. Synthesis of 4,7-dibromobenzothiadiazole

The synthetic route of 4,7-dibromobenzothiadiazole (BTd) was published previously [44]. In a three neck flask, BTd (5.0 g, 36.73 mmol) was dissolved using HBr (90 mL) as a solvent. Br_2 (4ml) and HBr (37.5 mL) were mixed and added to the BTd-HBr solution drop wise. After the addition was complete, the mixture was put into reflux for 12 hours. The mixture precipitated while it was cooled to room temperature. The precipitate was filtered and washed with saturated NaHSO_3 . This provides the extraction of excess bromine. The washed precipitate was dissolved in dichloromethane (DCM) and an extraction took place. The organic residue was dried over MgSO_4 . The solvent was removed under vacuum. The crude product was a yellow solid obtained with 90% yield. (9.75g, 33.05 mmol). ^1H NMR (400 MHz, CDCl_3) δ (ppm) 7.66 (s, 2H). ^{13}C NMR (101 MHz, CDCl_3) δ (ppm) 152.9, 132.3, 113.9.

2.3.2. Synthesis of 3,6-Dibromobenzene-1,2-diamine (2)

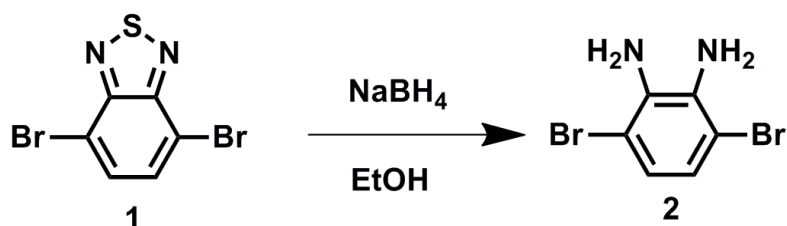


Fig. 2.2. Synthesis of 3,6-dibromobenzene-1,2-diamine

The synthetic route of 3,6-dibromobenzene-1,2-diamine was published previously [45]. In a 1000 ml flask, 4,7-Dibromobenzothiadiazole (1) (10.2 g, 34.70 mmol) was dissolved in ethanol (EtOH) (340 ml). NaBH_4 (24.4 g, 0.64 mol) was weighed carefully, preventing any air contact. The weighed NaBH_4 was added to the mixture in an ice bath in 4 hours. The mixture was stirred for 12 hours at

room temperature. The solvent was removed under vacuum. The remnant was dissolved in diethyl ether. Extraction was carried out. Organic phase was dried over MgSO_4 and the solvent was removed under vacuum. The crude product was a pale yellow solid obtained with 87% yield (8.0 g, 30.18 mmol). ^1H NMR (400 MHz, CDCl_3) δ (ppm) 6.78 (s, 2H), 3.82 (s, 4H). ^{13}C NMR (101 MHz, CDCl_3) δ (ppm) 133.5, 123.2, 109.5.

2.3.3. Synthesis of 4, 7-Dibromo-4'-(tert-butyl)spiro[benzo[d]imidazole-2,1'-cyclohexane] (3)

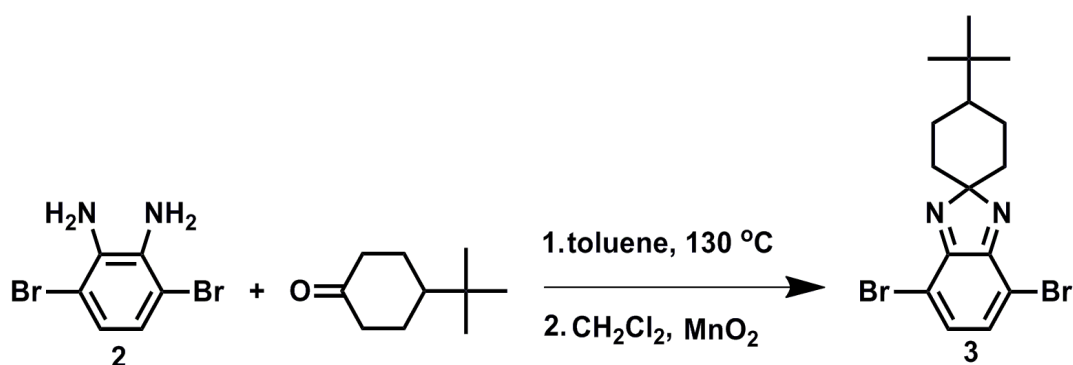


Fig. 2.3. Synthesis of 4, 7-dibromo-4'-(tert-butyl)spiro[benzo[d]imidazole-2,1'-cyclohexane]

3,6-Dibromobenzene-1,2-diamine (300 mg, 1.13 mmol), 4-tert-butylcyclohexanone (174 mg, 1.13 mmol) and toluene (8 ml) were mixed at 130°C for 24 hours under argon (Ar) atmosphere. The solvent of the solution was removed under vacuum. The remaining solid was dissolved in DCM (11ml) and stirred under argon atmosphere at room temperature. 85 % activated manganese (IV) oxide (800 mg, 9.16 mmol) was added to the solution. The mixture was stirred for 4 hours at room temperature and filtered. The filtered mixture was diluted with dichloromethane (80 ml), washed with distilled water (80 ml) 3 times and dried over MgSO_4 . The solvent was removed under vacuum. The crude product was purified by column chromatography (hexane:ethylacetate(10:1)). 4,7-Dibromo-4'-(tert-butyl)spiro[benzo[d]imidazole-2,1'-cyclohexane] was a yellow oily liquid, obtained with a 55% yield (249mg, 0.622 mmol). ^1H NMR (400 MHz, CDCl_3) δ (ppm) 7.12 (s, 2H), 2.25(t, 2H), 2.10 (m, 1H), 1.70 (t, 2H), 1.60(t, 2H), 1.30(t, 2H), 0.90(s, 9H) ^{13}C NMR (101 MHz, CDCl_3) δ (ppm) 157.00, 156.70, 135.80, 135.60, 119.30, 107.50, 107.50, 107.45, 47.80, 47.85, 47.80, 32.50, 35.80, 35.75, 27.75, 25.7

2.3.4. Synthesis of 2,5-Bis(tributylstannyl)thiophene

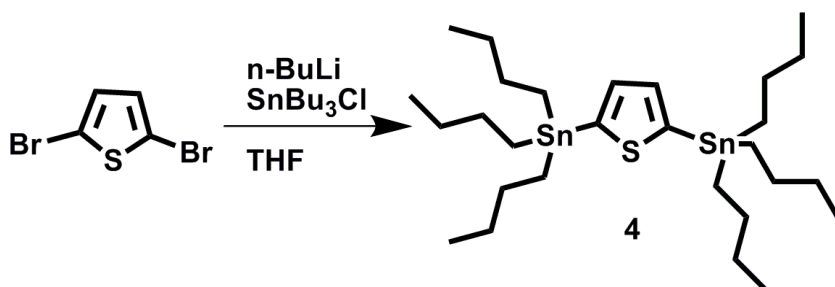


Fig. 2.4. Synthesis of 2,5-bis(tributylstannyl)thiophene

The synthesis of 2,5-bis(tributylstannyl)thiophene was published previously [47]. In a three neck flask, 2,5-dibromothiophene (7.26g, 30 mmol) was dissolved in dry THF (150 ml) under Ar atmosphere. *n*-Butyl lithium (32 mL 2.5 M in hexane, 80 mmol) was added drop wise at -78°C . The solution was stirred for 1 hour while maintaining the temperature at -78°C . $\text{Sn}(\text{Bu})_3\text{Cl}$ (32 ml, 120 mmol) was added at one portion. After stirring for 24 h at room temperature, the mixture was poured into 100 ml cooled water and an extraction was carried out by using hexane. The organic phase was dried over MgSO_4 . The solvent was removed under vacuum. The product is obtained as a yellowish-brown oily liquid with 83% yield. ^1H NMR (400 MHz, CDCl_3) δ (ppm) 7.39 (s, 1H), 1.62-1.53 (m, 12H), 1.38-1.29 (m, 12H), 1.13-1.08 (m, 12H), 0.94-0.84 (m, 18H).

2.3.5. Chemical Polymerization of P1

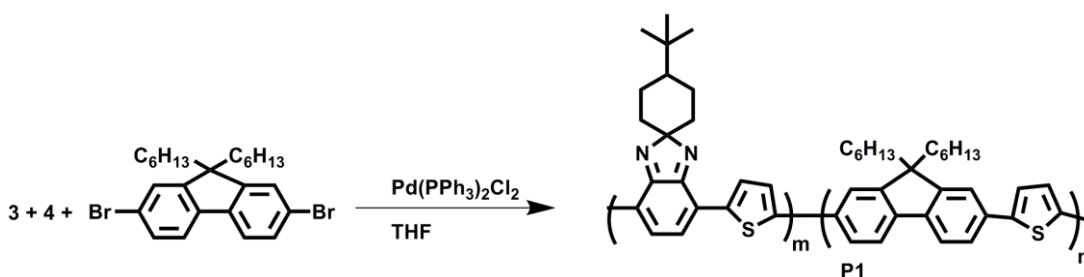


Fig. 2.5. Chemical Polymerization of P1

1 mol of 4, 7-dibromo-4'-(tert-butyl)spiro[benzo[d]imidazole-2,1'-cyclohexane] (3), 2 moles of 2,5-bis(tributylstannyl)thiophene and one mol of 2,7-dibromo-9,9-dihexyl-9H-fluorene were dissolved in dry THF under Ar atmosphere. The solution was heated to reflux. $\text{Pd}(\text{PPh}_3)_2\text{Cl}_2$ (5 mol%) was added under high argon flow and the mixture is refluxed for 48 hours. At the end of 48 h, the THF was

removed under vacuum and the precipitate was washed with methanol, hexane and acetone respectively using soxhlett apparatus. P1 was obtained as a dark green solid. (M_n : 4235 M_w : 35180 PDI: 8.3)

2.3.6. Chemical Polymerization of P2

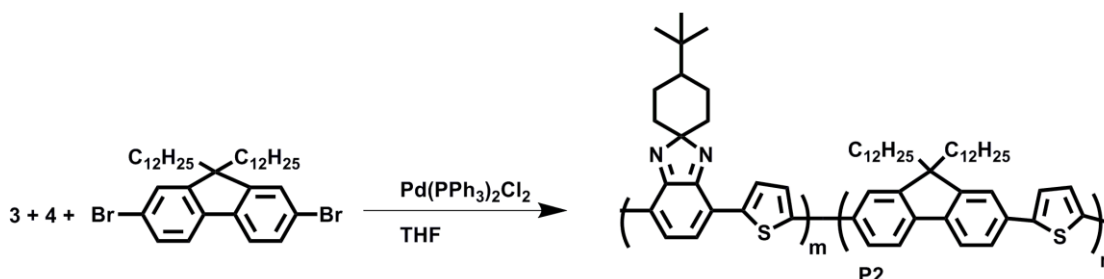


Fig. 2.6. Chemical Polymerization of P2

1 mol of 4, 7-dibromo-4'-(tert-butyl)spiro[benzo[d]imidazole-2,1'-cyclohexane] (3), 2 moles of 2,5-bis(tributylstannyl)thiophene and one mol of 2,7-dibromo-9,9-didodecyl-9H-fluorene were dissolved in dry THF under Ar atmosphere. After the solution was heated to reflux, Pd(PPh₃)₂Cl₂ (5 mol%) was added under high argon flow. The mixture was refluxed for 48 hours. At the end of 48 h, the THF was removed under vacuum and the precipitate was washed with methanol, hexane and acetone respectively using soxhlett. P1 was obtained as a dark green solid. (M_n : 6725 M_w : 49125 PDI: 7.3)

2.4. Characterization of Conducting Polymers

A special technique must be applied for the characterization of conducting polymers, as the conjugated polymers may have solubility problems. Cyclic voltammetry is one of these special techniques. It is used to obtain some qualitative information about the electrochemical reactions taking place on the polymer. Secondly, spectroelectrochemistry is used to identify the changes occurring on the doped conducting polymer. Information about polaron and bipolaron bands is obtained by this technique. Kinetic studies are also conducted in order to characterize a conjugated polymer examining the switching time and color change.

2.4.1. Cyclic Voltammetry

In this method, the potential of the stationary working electrode, immersed in an unstirred solution is cycled by triangular waves and the generated current is measured. The cycle is between the times where no electrochemical reaction takes place and when redox reactions take place. The applied

potential is measured by a potentiostat. Figure 2.7 shows the voltage change as a function of time and Figure 2.8 shows the expected current change as a function of voltage.

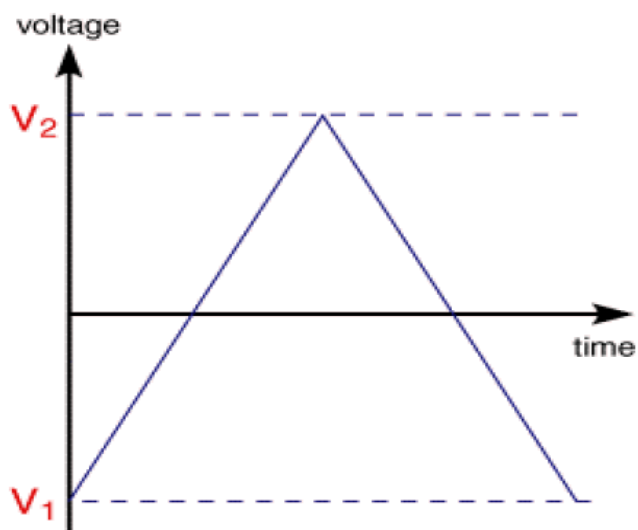


Fig. 2.7. Voltage change as a function of time

The peaks in the CV depend on the diffusion behavior on the electrode surface. As the concentration gradient change with time, the peaks are either formed or disappeared. This phenomenon is described in Randles-Sevcik equation;

$$i_p = k n^{3/2} v^{1/2} D^{1/2} A C$$

The peak height i_p is directly proportional to the concentration C . n is the number of electrons of the half cell reactions for the redox couple, v is the scan rate (V/s), D is the diffusion coefficient (cm^2/s) and A is the electrode area (cm^2) in this equation.

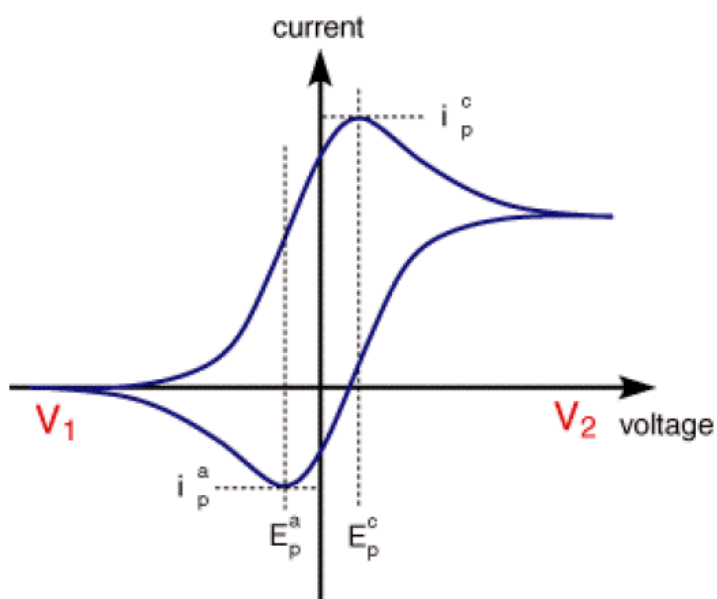


Fig. 2.8. Voltage change as a function of current

In cyclic voltammetry, a three electrode system is used. A working electrode, a counter electrode and a reference electrode are involved. By using the working and reference electrode, the potential is calculated and by using the working and counter electrode, the current is calculated (Fig. 2.9). In this study, electrochemical properties of the polymers are investigated by cyclic voltammetry.

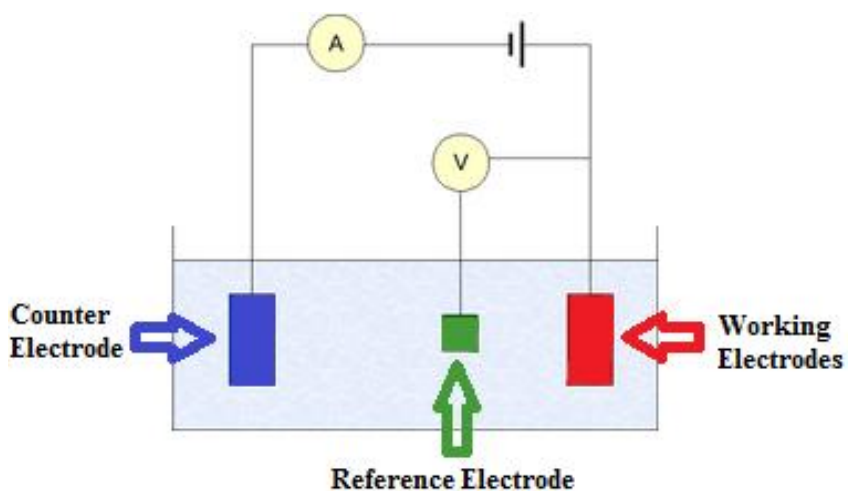


Fig. 2.9. Three electrode system

2.4.2. Spectroelectrochemistry

Spectroelectrochemical studies involve the combination of spectroscopy and electrochemistry. The polymer is coated on an ITO coated glass by spray coating in order to be characterized by spectroelectrochemistry.

A potentiostat, a UV-vis-nIR spectrophotometer and a three electrode system are coupled in spectroelectrochemical studies. Optical properties of the polymer can be studied in addition to investigating the polaronic and bipolaronic states. The optical band gap, electronic transitions and absorption spectra can also be obtained by this method.

2.4.3. Colorimetry

In order to define the color and contrast ratio of the synthesized electrochromic polymers, in-situ colorimetry technique is used. In this technique, the color is defined more precisely than in spectrophotometry. It is a way of measuring and expressing the color according to the sensitivity of the human eye towards light in the visible region. The colors can be measured from neutral to doped states quantitatively. The expression of color depends on some coordinates such as the CIE 1931 Lab color space. Referring to the coordinates enables the global scientific designation of that specific tone of that specific color.

In the CIE 1931 Lab color space, three coordinates are used. "L" stands for the brightness of the color (luminance). "a" defines the hue of the color which is the wavelength that has the maximum contrast (dominant wavelength). Finally, "b" is the intensity of the color (saturation).

2.4.4. Kinetic Studies

Kinetic studies were performed in order to identify the optical contrast (or percent transmittance) of the electrochromic material as a function of time. The difference in transmittance between the neutral and fully doped states is measured at the λ_{\max} values giving potential to every state in periods of 5 sec.

A three electrode system, a potentiostat and a UV-vis-nIR spectrophotometer were involved in kinetic studies. Polymers were coated on an ITO surface by spray coating. A square wave potential between the neutral and fully doped states was given to the substrate for 5 seconds at the λ_{\max} values in a monomer free environment with an electrolyte/solvent couple of $\text{NaClO}_4\text{-LiClO}_4/\text{ACN}$. The optical contrast and switching time values were obtained this way.

CHAPTER 3

RESULTS AND DISCUSSION

3.1. Electrochemical Characterization of Polymers

Polymers P1 and P2 were characterized by cyclic voltammetry. The scan rate dependence of the processes was investigated. The electroactivity and the HOMO levels were measured using thin films of polymers inserted in a three electrode system. Measurements were done in a monomer free environment. NHE was taken as -4.75 eV vs. vacuum and HOMO levels were calculated from the onset of the corresponding oxidation potentials against Fc/Fc^+ reference electrode.

3.1.1. Cyclic Voltammogram of P1

Cyclic voltammetry of P1 was performed in a monomer free environment with a 0.1 M NaClO_4 - $\text{LiClO}_4/\text{ACN}$ solution. The voltammogram can be seen in Figure 3.1. A reversible p-doping peak appears at 1.1 V/ 0.8 V. Drawing a tangent to the onset of this peak, the HOMO energy level was calculated as -5.67 eV. As the polymer was not n-dopable, the LUMO energy level could not be calculated directly from the voltammogram.

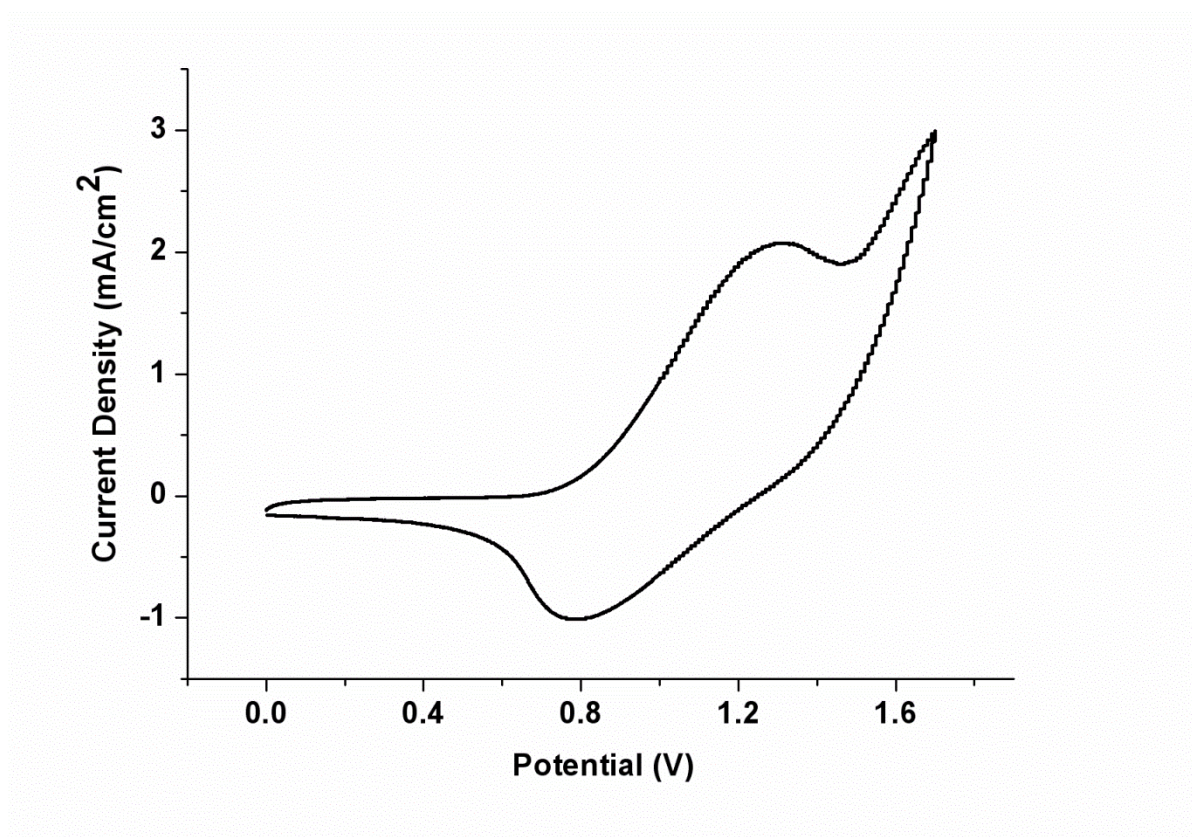


Fig. 3.1. Cyclic Voltammogram of P1 which was taken in a monomer free environment with a 0.1 M $\text{NaClO}_4\text{-LiClO}_4/\text{ACN}$ solution.

3.1.2. Scan Rate Dependence of P1

The scan rate dependence of P1 was measured by CV. A linear dependence of peak current to the scan rate was observed. This shows that the polymer films were successfully adhered and electro-active, providing a proof for non-diffusion controlled reversible oxidation process for P1 [48].

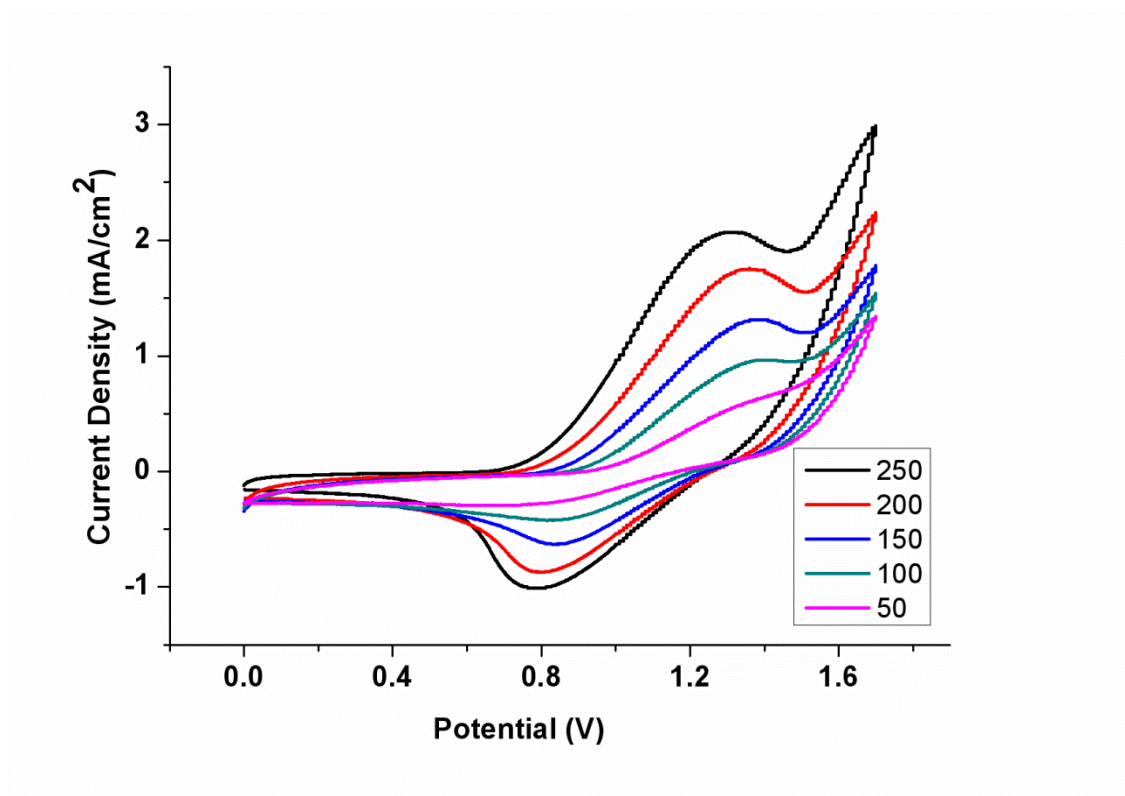


Fig. 3.2. Scan rate dependence of P1 film in a 0.1 M NaClO₄-LiClO₄/ACN solution.

3.1.3. Cyclic Voltammogram of P2

Cyclic voltammogram of P2 can be seen in Figure 3.2. Cyclic voltammetry was performed in a monomer free environment with a 0.1 M NaClO₄-LiClO₄/ACN solution. A reversible p-doping peak appears at 1.3 V/ 1.1 V. From the onset of this peak, the HOMO energy level was calculated as -5.89 eV. Due to the lack of n-dopability, the LUMO level of P2 could not be calculated directly from the cyclic voltammogram.

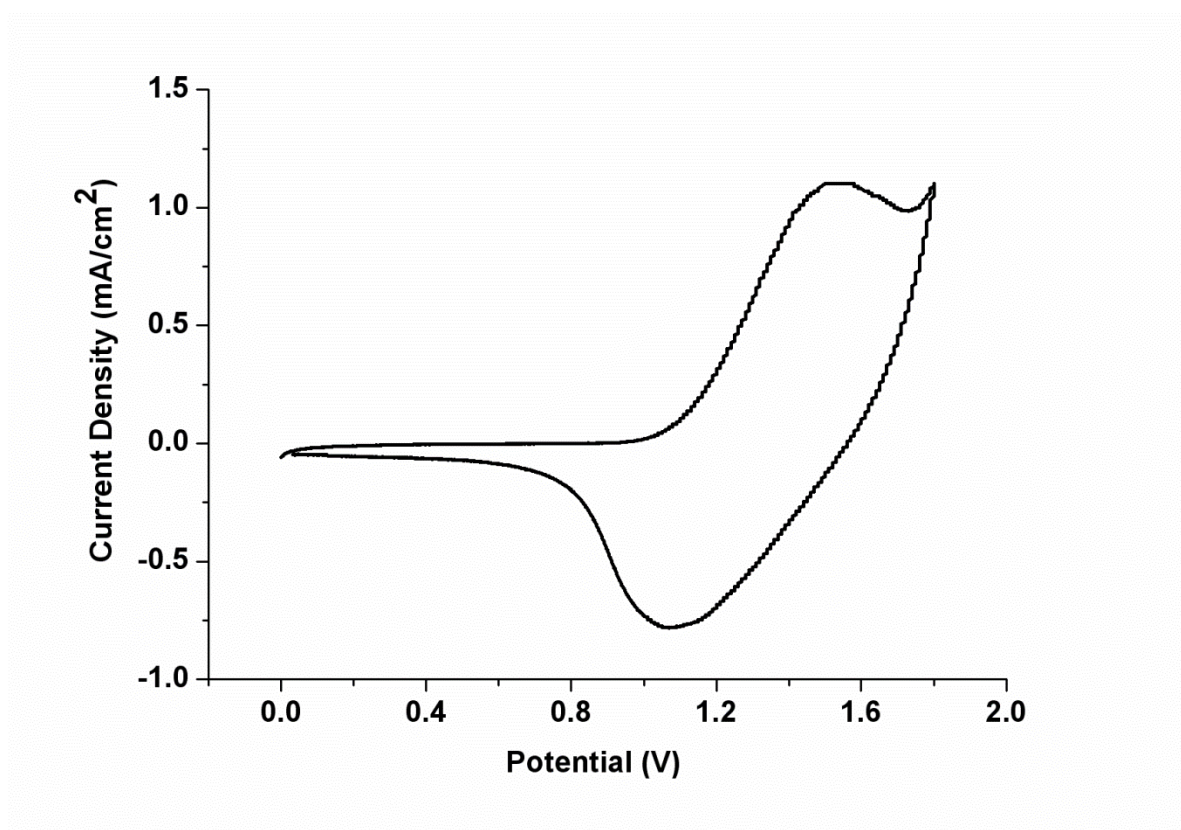


Fig. 3.3. Cyclic Voltammogram of P2 which was taken in a monomer free environment with a 0.1 M NaClO₄-LiClO₄/ACN solution.

3.1.4. Scan Rate Dependence of P2

The CV in Figure 3.4. shows the scan rate dependence of anodic peak current for P2. The resulting linear dependence provides explanation for the successfully adhered electroactive film of P2. This proves the presence of a non-diffusion controlled reversible oxidation process for P2 [49].

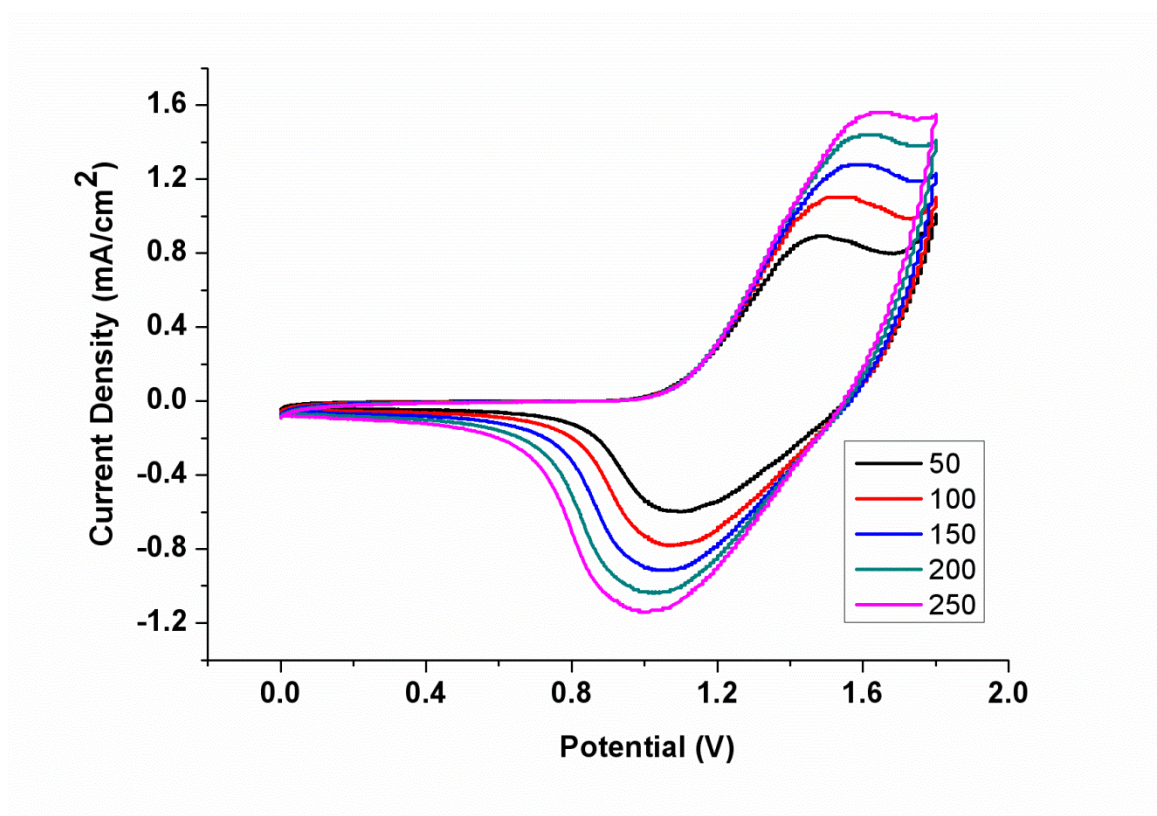


Fig. 3.4. Scan rate dependence of P2 film in a 0.1 M NaClO₄-LiClO₄/ACN solution.

3.2. Spectroelectrochemistry Studies

Spectroelectrochemistry studies were held in order to observe the changes in optical properties of the polymer upon doping. Polymers were coated on ITO coated glass slides. Spectroelectrochemistry studies were held in a 0.1 M NaClO₄-LiClO₄/ACN solution in order to investigate the absorption behavior of the polymers. Charge carrier bands appeared as a consequence of p-doping. The potential was increased stepwise with 100 mV intervals, considering the pre-determined oxidation potentials. A range of 0-1.8 V was investigated. Optical band gaps were calculated and by assuming the equivalence of optical and electronic band gaps, LUMO levels were calculated by using previously determined HOMO levels.

3.2.1. Spectroelectrochemistry Studies for P1

P1 has two distinctly separated absorption maxima around 425 and 625 nm which is essential for its green color (L: 62.254, a: -40.559, b: 46.918). The optical band gap (E_g^{op}) of P1 was calculated by

drawing a tangent to the onset of the second π - π^* transition. By using De Broglie equation, the band gap was found as 2.46 eV. Assuming the optical (E_g^{op}) and electronic (E_g^{el}) band gaps to be equal, the LUMO of P1 was found as -3.21 eV by taking the difference between the electronic band gap and the previously calculated HOMO level.

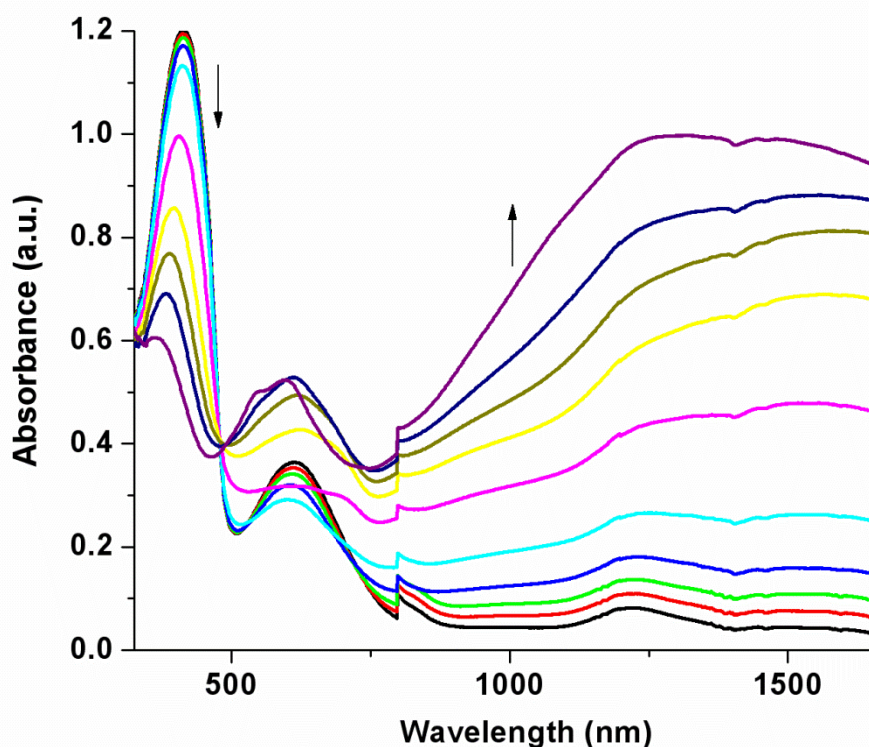


Fig. 3.5. Spectroelectrochemistry of P1 film on an ITO coated glass slide in monomer-free, 0.1 M NaClO₄-LiClO₄/ACN electrolyte-solvent couple at applied potentials (from 0 to 1.8V).

Oxidation of P1 film leads to a decrease of both absorption bands in the visible region but the decrease in the first absorption band at 425 nm is more obvious than the second π - π^* transition. Simultaneously with this decrease, a new absorption band in the NIR region appears. The formation of this new band is due to the formation of charge carriers on the polymer backbone. If the decrease of the absorption bands were at equal amounts, the oxidized state of the polymer would turn out to be transparent [50]. In our case, as the decrease in the second π - π^* which is at the blue region of the visible spectra is less, the dominant absorption band of the oxidized polymer is also at the blue region. This causes the oxidized polymer appear blue.

In order to express the color of the oxidized polymer scientifically, colorimetry study is held. P1 is a neutral state green polymer (L: 62.254, a: -40.559, b: 46.918). The transition states of P1 had absorption that revealed yellowish green and grayish blue colors respectively (L: 67.799, a: -18.276, b: 56.694 and L: 53.707, a: -26.353, b: 14.452). Oxidized state of P1 shows blue color (L: 49.130, a: -4.447, b: -21.784)

For the last 30 years, the synthesized conducting polymers revealed either blue or red color in their neutral state. Neutral state green polymer was missing. By synthesizing red, blue and green colored polymers, all spectrum colors can be obtained. So it became a necessity to synthesize a neutral state green polymer. In 2004, Sonmez et. al. synthesized the first neutral state green polymer [51] which was brown in its doped state. In 2009, our research group synthesized the first neutral state green polymer that has a transmissive doped state [50]. In the light of all these, in synthesizing a neutral state green polymer is a very important contribution to the literature.

0.0 V	1.1 V	1.3 V	1.5 V
			
L:62.254 a:-40.559 b:46.918	L:67.799 a:-18.276 b:56.694	L:53.707 a:-26.353 b:14.452	L:49.130 a:-4.447 b:-21.784

Fig. 3.6. L.a.b colors of P1 on an ITO coated glass slide in the neutral and oxidized states.

3.2.2. Spectroelectrochemistry Studies for P2

P2 also revealed green color due to its two distinct absorption maxima in the visible region; both at 445 nm and 625 nm (L: 67.576, a: -32.549, b: 54.600). From the onset of the absorption band with longer wavelength and by using De Broglie equation, the optical band gap (E_{g}^{op}) was calculated as 2.54 eV. By taking the difference between the previously calculated HOMO level and the electronic band gap, (electronic band gap was assumed to be equal with the optical band gap), LUMO level of P2 was found to be -3.35 eV.

With oxidation of P2, the intensity of the first neutral state absorption band decreases drastically. A new absorption band appears in the NIR region due to the charge carriers. As the decrease in the second neutral state absorption band is less than the first one, the dominant color upon oxidation is blue.

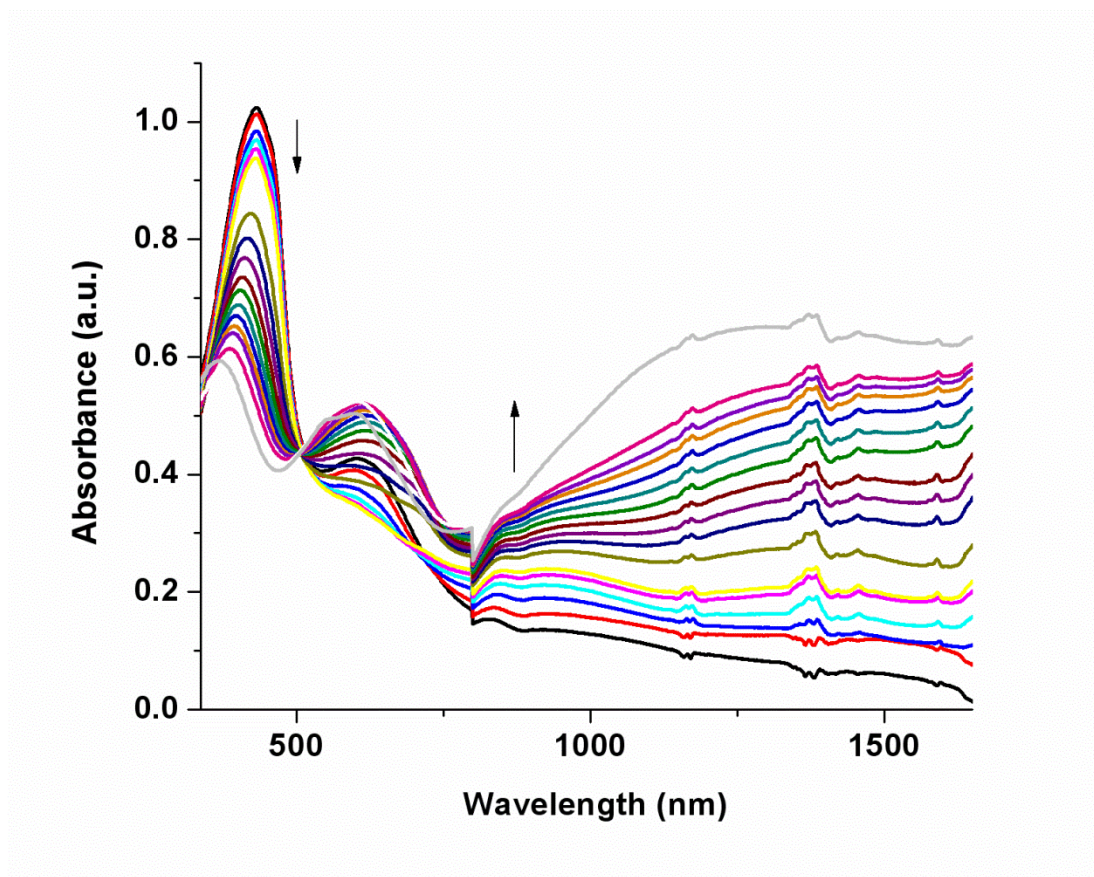


Fig 3.7. Spectroelectrochemistry of P2 film on an ITO coated glass slide in monomer-free, 0.1 M NaClO₄-LiClO₄/ACN electrolyte–solvent couple at applied potentials (from 0 to 1.8V).

P2 showed grey color (L: 45.221, a: -7.112, b: 9.246) as the absorption tail of the polaron band was placed adjacent to the visible region border. The fully oxidized P2 revealed blue color (L: 43.800, a: -1.134, b: -21.846).

Both polymers revealed neutral state green and oxidized state blue colors. Their neutral state green color provides importance for further applications.

0.0 V	1.2 V	1.4 V
		
L:67.576 a:-32.549 b:54.600	L:45.221 a:-7.112 b:9.246	L:43.800 a:-1.134 b:-21.846

Fig. 3.8. L.a.b. colors of P2 film on an ITO coated glass slide in the neutral and oxidized states.

3.3. Kinetic Studies

The switching times of polymers P1 and P2 at their λ_{\max} values and the percent transmittance changes in accordance with time were measured in kinetic studies. The measurement was done between the neutral and fully oxidized states of the polymers by giving potentials for 5 sec. The time needed for the polymer to perform a switch between their neutral and oxidized states were measured.

3.3.1. Kinetic Study of P1

At 410 nm, P1 showed 32% transmittance change with a switching time of 2.5 s. With a 30% transmittance change, P1 had a switching time of 1.7 s at 1310 nm. This revealed that the transmittance values are better for P1 in the visible region although its switching time is better in IR region.

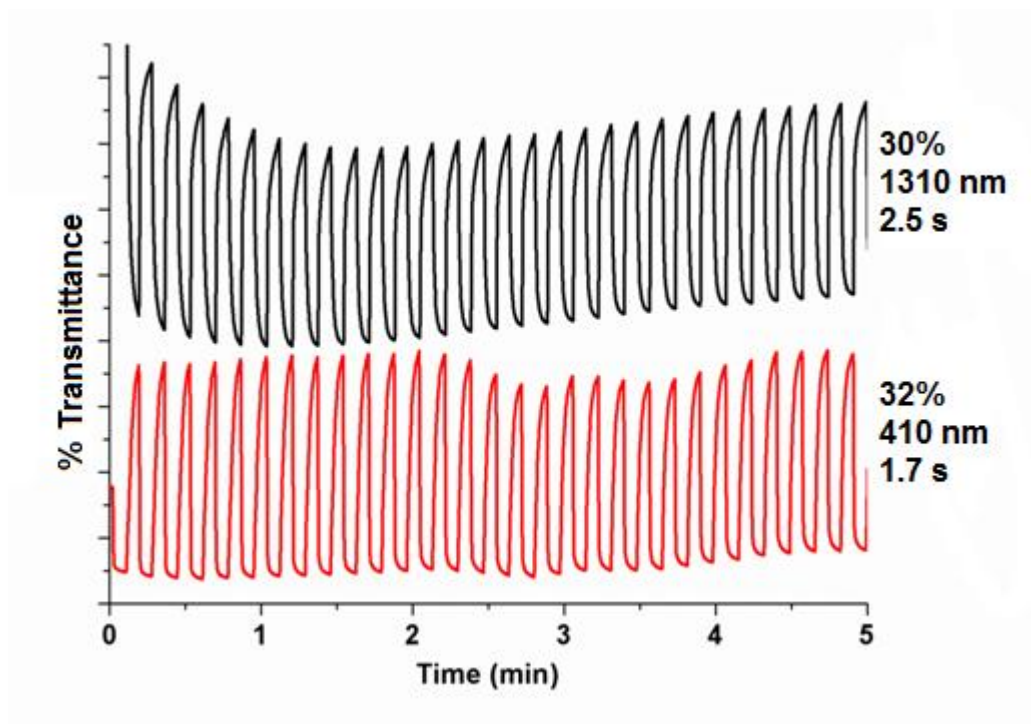


Fig 3.9. Percent transmittance change and switching times for P1 monitored at 410 and 1310 nm in 0.1 M NaClO₄-LiClO₄/ACN electrolyte–solvent couple.

3.3.2. Kinetic Study of P2

The percent transmittance change of P2 at 445 nm was measured to be 25% with a high switching time of 3.2 s. However at 1320 nm, the percent transmittance change was raised to 53% and the switching time is 1.1 s. This reveals the fact that P2 Shows better results in kinetic studies held in IR region.

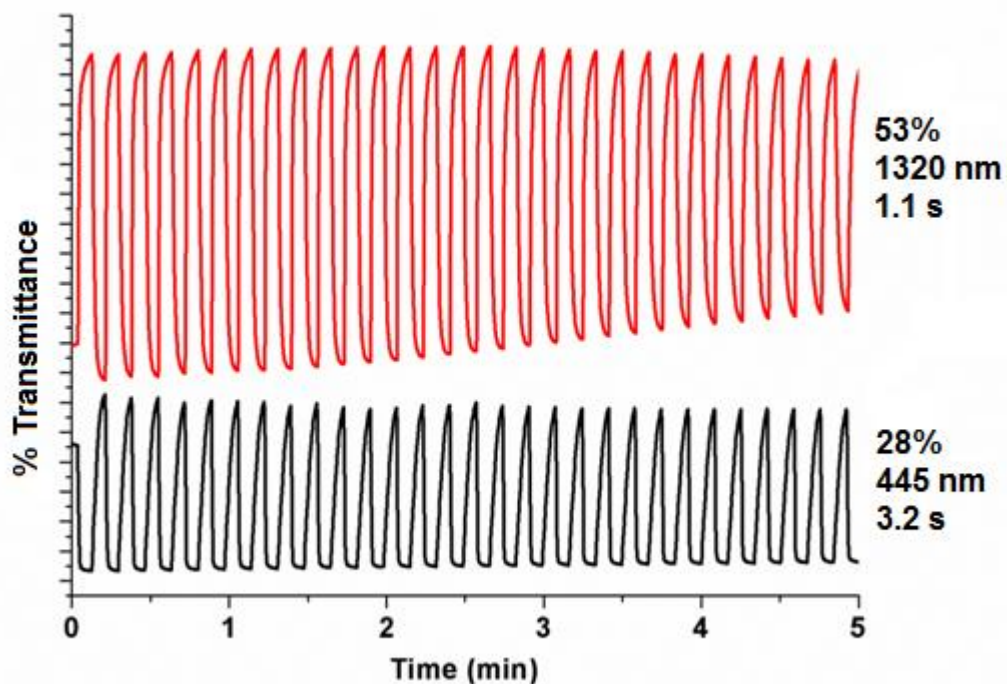


Fig. 3.10. Percent transmittance change and switching times for P2 monitored at 445 and 1320 nm in 0.1 M NaClO₄-LiClO₄/ACN electrolyte–solvent couple.

3.4 Summary of Results and Comparison of Polymers

Table 1. Summary of Results

	E_{doping}	$E_{\text{de-doping}}$	HOMO	LUMO	E_g^{op}
P1	1.1 V	0.8 V	-5.67 eV	-3.21 eV	2.46 eV
P2	1.3 V	1.1 V	-5.89 eV	-3.35 eV	2.54 eV

When P1 and P2 are compared in terms of their oxidation potentials, it is easier for P1 to get oxidized. The increase in the alkyl chain length in the fluorene units causes steric bulkiness and this makes it harder to be oxidized.

None of the polymers were n-dopable which was caused by the electron rich nature of the repeating unit. Due to their lack of ability in n-doping, the LUMO levels cannot be calculated from cyclic voltammograms. As a solution, the optical and electronic band gaps were assumed to be equal and the LUMO levels were calculated by using the optical band gaps and HOMO levels.

The criteria for a neutral state green polymer is to have two absorption bands in the visible range. One in red and one in blue region. Both polymers satisfy this criteria. P1 had absorption in 410 nm and 610 nm and P2 had absorption at 445 and 612 nm. Both polymers were neutral state green polymers. It is important to synthesize a neutral state green polymer as it was the missing color for applications using RGB colors until recent years. In year 2004 Sonmez et. Al. managed to synthesize the neutral state green polymer and in 2009 our research group synthesized the first neutral state green-doped state transparent polymer. With this knowledge, to synthesize a processible neutral state green polymer is an important contribution.

The increase of chain length of alkyl chain attached to the fluorene unit increased the solubility and processibility of the polymer, leading to a higher variety of application possibilities. On the other hand, the band gap of P2 is slightly higher than P1 due to this alkyl chain length increase. The increase in steric bulky groups caused a decrease in effective π overlapping and this causes a decrease in effective conjugation. Also the bulkiness causes some distortion from planarity. All these effects lead to the increase in band gap of P2.

CHAPTER 4

CONCLUSION

Two fluorene and benzimidazole containing polymers were synthesized electrochemically. Cyclic voltammetry, spectroelectrochemistry and kinetic studies were used in order to characterize the polymers.

Spectroelectrochemistry studies revealed the two π - π^* transitions of the polymers, resulting in green color. Both were neutral state green polymers. The neutral state, transition state and doped state colors were expressed in terms of L.a.b. values. The bands were found to be 2.46 and 2.54 respectively for P1 and P2. The increase in alkyl chain length caused the solubility and processibility of the polymer to increase and also the band gap of the polymer to raise by decreasing the effective conjugation and planarity. In cyclic voltammetry, it was seen that the oxidation of P1 is easier than P2 due to the shorter alkyl chain in fluorene moieties. The polymers were p- dopable but they were not n-dopable. Both polymers were multichromic. This study have shown that both polymers have distinctive π - π^* transitions, band structure, and backbone that provides oxidative doping.

REFERENCES

- [1] H. Letheby, *J. Chem. Soc.*, **1862**, 15, 161.
- [2] A. J. Heeger, *Angew. Chem. Int. Ed.*, **1976**, 40, 2591.
- [3] H. Shirakawa, E. J. Louis, A. G. MacDiarmid, C. K. Chiang, A. J. Heeger, *Chem. Commun.*, **1977**, 578.
- [4] (a) H. Shirakawa, *Angew. Chem. Int. Ed.*, **2001**, 40, 2574. (b) A. G. MacDiarmid, *Angew. Chem. Int. Ed.*, **2001**, 40, 2581. (c) A. J. Heeger, *Angew. Chem. Int. Ed.*, **2001**, 40, 2591. (d) H. Shirakawa, *Synth. Met.*, **2002**, 125, 3. (e) A. G. MacDiarmid, *Synth. Met.*, **2002**, 125, 11. (f) A. J. Heeger, *Synth. Met.*, **2002**, 125, 23.
- [5] A. Cirpan, S. Alkan, L. Toppare, Y. Hepuzer, Y. Yağcı, *J. Polym. Sci. Polym. Chem.*, **2002**, 40, 4131.
- [6] A. Cirpan, S. Alkan, L. Toppare, I. Cianga, Y. Yagci, *Designed Monomers & Polymers*, **2003**, 6, 237.
- [7] A. Gandini, M. N. Belgancem, *Prog. Polym. Sci.*, **1997**, 22, 1203.
- [8] (a) A. G. Bayer Eur. Patent 339,340, 1988 (b) F. Jonas, L. Schrader, *Synth. Met.*, 1991, 41, 831. (c) G. Heywang, F. Jonas, *Adv. Mater.*, **1992**, 4, 116.
- [9] (a) A. F. Diaz, K. K. Kanazawa, G. P. Gardini, *J. Chem. Soc., Chem. Commun.*, 1979, 635. (b) A. F. Diaz, J. I. Castillo, J. A. Logan, W. Lee, *J. Electroanal. Chem.*, 1981, 129, 115. (c) K. Lee, A. J. Heeger, *Synth. Met.*, **1997**, 84, 715.
- [10] G. Grem, G. Leditzky, B. Ullrich, G. Leising, *Adv. Mater.*, **1992**, 4, 36.
- [11] J. H. Burroughes, D. D. C. Bradley, A. R. Brown, R. N. Marks, K. MacKay, R. H. Friend, P. L. Burn, A. B. Holmes, *Nature*, **1990**, 347, 539.
- [12] J. Rault-Berthelot, J. Simonet, *J. Electrochem. Soc.*, **1985**, 182, 187.
- [13] A. G. MacDiarmid, A. J. Epstein, *Farad. Discuss. Chem. Soc.*, **1989**, 88, 317.
- [14] A. Desbene-Monvernay, P.-C. Lacaze, J.-E. Dubois, *J. Electroanal. Chem.*, **1981**, 129, 229.
- [15] Salzner U, Lagowski JB, Pickup PG, Poirier RA. *Synth. Met.*, **1998**, 96, 177.
- [16] M. G. Kanatzidis, *Chem. Eng. News.*, **1990**, 68, 36.
- [17] P. Chandrasekhar, *Conducting Polymers Fundamentals and Applications*, Boston, Kluwer Academic Publishers, **1999** Ch. 2
- [18] A. G. MacDiarmid, A. J. Heeger, *Synthetic Metals*, **1979**, 1, 101.
- [19] J. I. Reddinger, J. R. Reynolds, *Adv. Polym. Sci.*, **1999**, 45, 59.

- [20] J. L. Bredas, G. B. Street, *Acc. Chem. Res.*, **1985**, 18, 309.
- [21] D. Baeriswyl, D. Campbell, S. Mazumdar, *Conjugated Conducting Polymers*, **1992**, 36, 195.
- [22] Varis, S., Ak, M., Tanyeli, C., Akhmedov, I.M., Toppare, L., *Eur. Polym. J.*, **2006**, 42, 2352.
- [23] (a) C. G. Granqvist, *Sol. Energy Mater. Sol. Cells*, 2000, 60, 201. (b) C. G. Granqvist, E. Avendano, A. Azens, *Thin Solid Films*, 2003, 442, 201. (c) B. W. Faughnan, R. S. Crandall, P. M. Heyman, *RCA Rev.*, **1975**, 36, 177.
- [24] D. R. Rosseinsky, R. J. Mortimer, *Adv. Mater.*, **2001**, 13, 783.
- [25] R.J. Mortimer, *Electrochimica Acta*, **1999**, 44, 2971.
- [26] Sonmez, G., Schwendeman, I., Schottland, P., Zong, K., Reynolds, J.R., *Macromolecules*, **2003**, 36, 639.
- [27] K. Fesser, A. R. Bishop, D. K. Campbell, *Phys. Rev. B*, **1983**, 27, 4804.
- [28] M. E Goppelsroder, *Compt. Rend.*, **1876**, 82, 331.
- [29] (a) A. F. Diaz, K. K. Kanazawa, G. P. Gardini, *Chem. Commun.*, 1979, 635. (b) A. F. Diaz, J. I. Castillo, *J. Chem. Soc. Chem. Commun.*, **1980**, 397.
- [30] G. A. Sotzing, J. L. Reddinger, A. R. Katritzky, J. Soloducho, R. Musgrave, J. R. Reynolds, *Chem. Mater.*, **1997**, 9, 1578.
- [31] D. Kumar, R. C. Sharma, *Eur. Poly. J.*, **1998**, 34, 1053.
- [32] Vadera S.R., Kumar N., Hwa Fuchen, in 1st International Conference on Frontiers of Polymer Research, Jan 20-25, New Delhi, **1991**.
- [33] Yoshino K., Hayashi R., Sugimoto R., *Jpn. J. Appl. Pyhs.*, **1984**, 23, 899.
- [34] P. J. Nigrey, A. G. MacDiarmid, A. J. Heeger, *J. Chem. Soc. Chem. Commun.*, **1979**, 594.
- [35] E. A. Meijere, F. Diederich, *Metal-Catalyzed Cross-Coupling Reactions*, Wiley-VCH, Weinheim, **2004**, (2).
- [36] J. K. Stille, *Angew. Chem., Int. Ed. Engl.*, **1986**, 25, 508.
- [37] J. Roncali, *Macromol. Rapid Commun.* **2007**, 28, 1761.
- [38] J. Roncali, *Chem. Rev.*, **1997**, 97, 173.
- [39] J.-L. Bre´das, *J. Chem. Phys.*, **1985**, 82, 3808.
- [40] F. Wudl, M. Kobayashi, A. J. Heeger, *J. Org. Chem.*, **1984**, 49, 3382.
- [41] E. E. Havinga, W. ten Hoeve, H. Wynberg, *Polym. Bull.* **1992**, 29, 119.
- [42] H.A.M. Mullekom, J.A.J.M. Vekemans, E.E. Havinga and E.W. Meijer, *Mater. Sci. Eng.*, **2001**, R32, 1.

- [43] T. Yamamoto, Z.H. Zhou, T. Kanbara, M. Shimura, K. Kizu, T. Maruyama, Y. Nakamura, T. Fukuda, B.L. Lee, N. Ooba, S. Tomaru, T. Kurihara, T. Kaino, K. Kubota, S. Sasaki, *J. Am. Chem. Soc.*, **1996**, 118, 10389.
- [44] J. Kim, S. Park, J. Kim, S. Cho, Y. Jin, J. Y. Shim, H. Shin, S. Kwon, I. Kim, K. Lee, A. J. Heeger, H. Suh, *JPSA*, **2011**, 49, 369.
- [45] A. B. Da Silveria Neto, A. L. Santana, G. Ebeling, S. R. Goncalves, E. V. U. Costa, H. F. Quina., Dupont J, *Tetrahedron*, **2005**, 61, 46, 10975.
- [46] Y. Tsubata, T. Suzuki, T. Miyashi, Y. Yamashita., *J. Org. Chem*, **1992**, 57, 25, 6749.
- [47] S.S. Zhu, T.M. Swager, *J. Am. Chem. Soc.* **1997**, 119, 12568.
- [48] A. Kumar, D. M. Welsh, M.C. Morvant, F. Piroux, K. A. Abbound, J.R. Reynolds, *Chem. Mater.*, **1998**, 10, 896.
- [49] G. Sonmez, I. Schwendeman, P. Schottland, K. Zong, J. R. Reynolds, *Macromolecules*, **2003**, 36, 639.
- [50] G. Gunbas, A. Durmus, L. Toppare, *Adv. Func. Mat.*, **2008**, 14, 2026.
- [51] G. Sonmez, C. K. F. Shen, Y. Rubin and F. Wudl, *Angew. Chem., Int. Ed.*, **2004**, 43, 1498.

APPENDIX

NMR DATA

Bruker DPX 400 was used to record NMR spectra.

Chemical shifts δ were reported in ppm relative to CHCl_3 (^1H : $\delta=7.27$), CDCl_3 (^{13}C : $\delta=77.0$) and CCl_4 (^{13}C : $\delta=96.4$) as internal standards.

The products had the following ^1H and ^{13}C NMR spectra

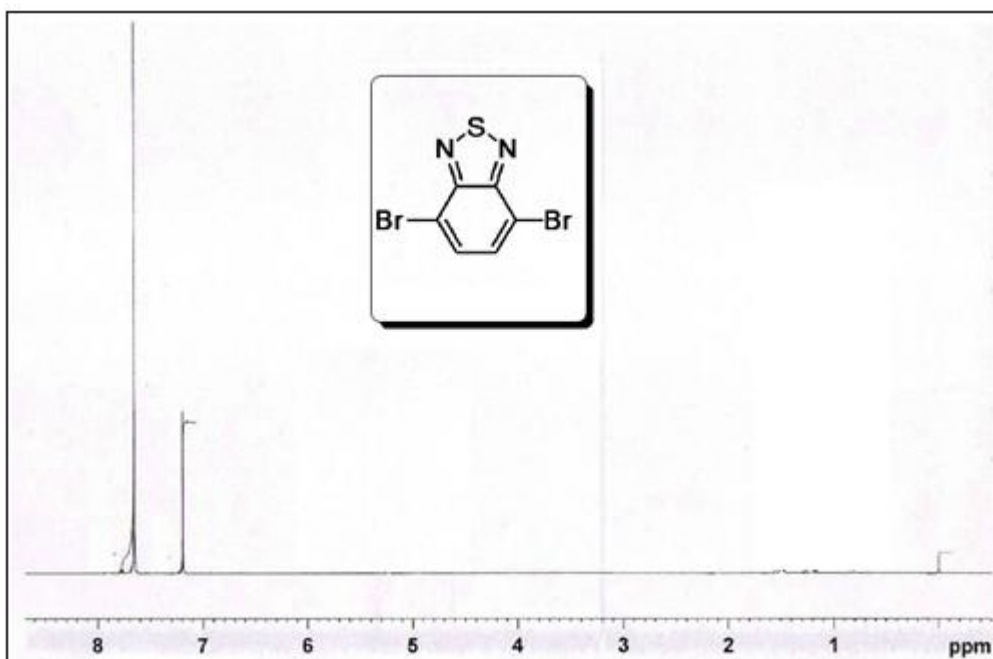


Fig. A. 1. ^1H -NMR spectrum of 4,7-dibromobenzothiadiazole (1)

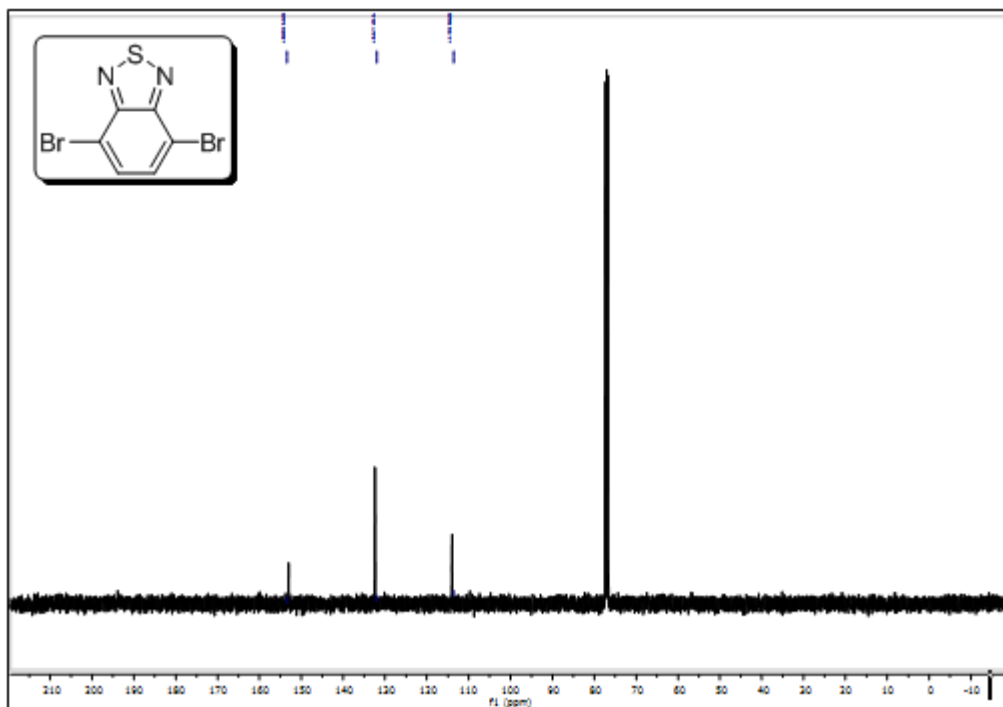


Fig. A. 2. ^{13}C -NMR spectrum of 4,7-dibromobenzothiadiazole (1),

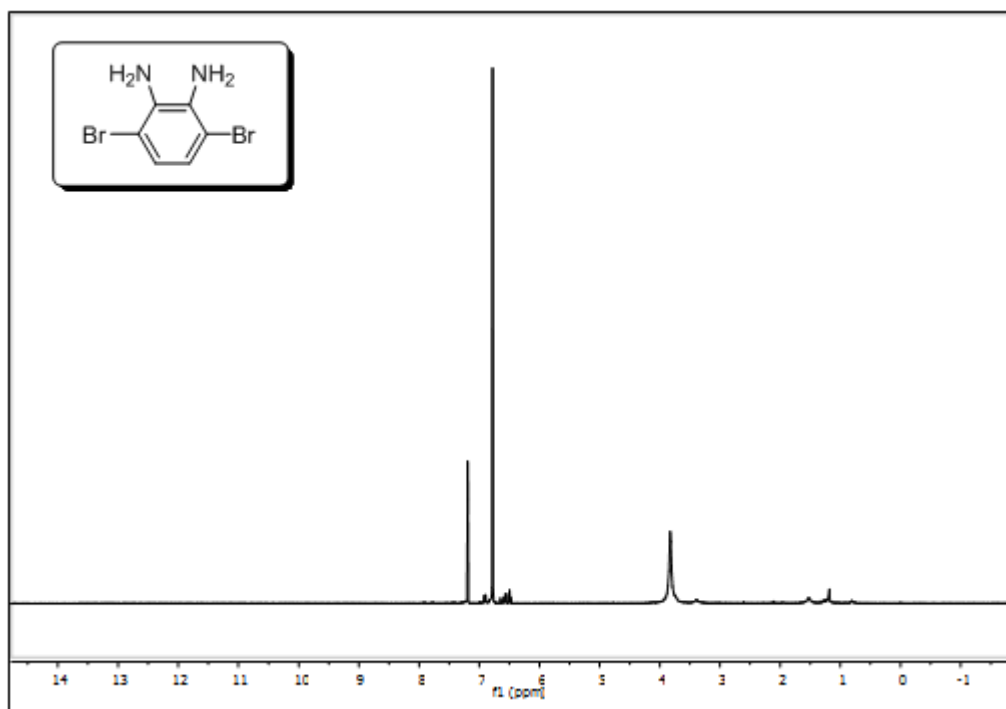


Fig. A. 3. ^1H -NMR spectrum of 3,6-dibromobenzene-1,2-diamine (2)

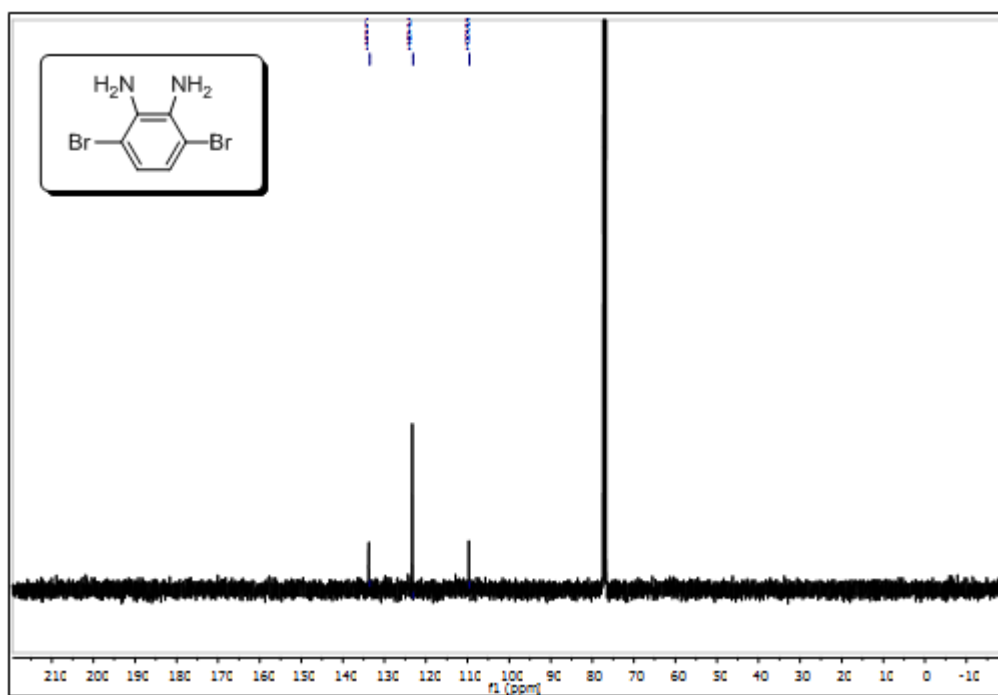


Fig. A. 4. ^{13}C -NMR spectrum of 3,6-dibromobenzene-1,2-diamine (2)

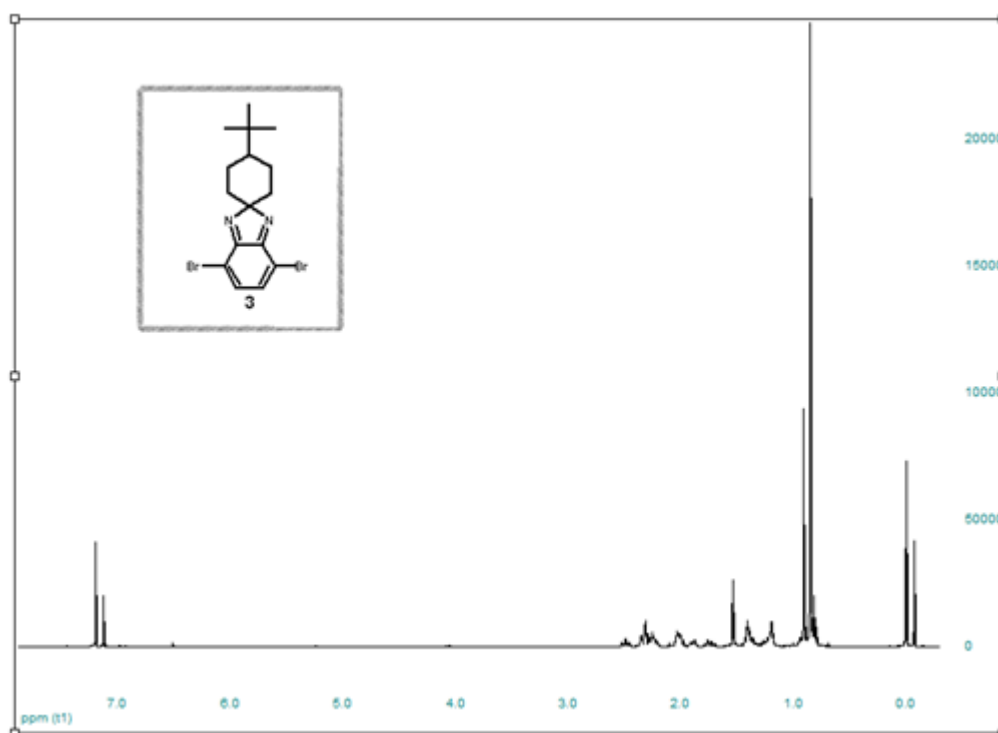


Fig. A. 5. ^1H -NMR spectrum of 4,7-dibromo-4'-(tert-butyl)spiro[benzo[d]imidazole-2,1'-cyclohexane] (3)

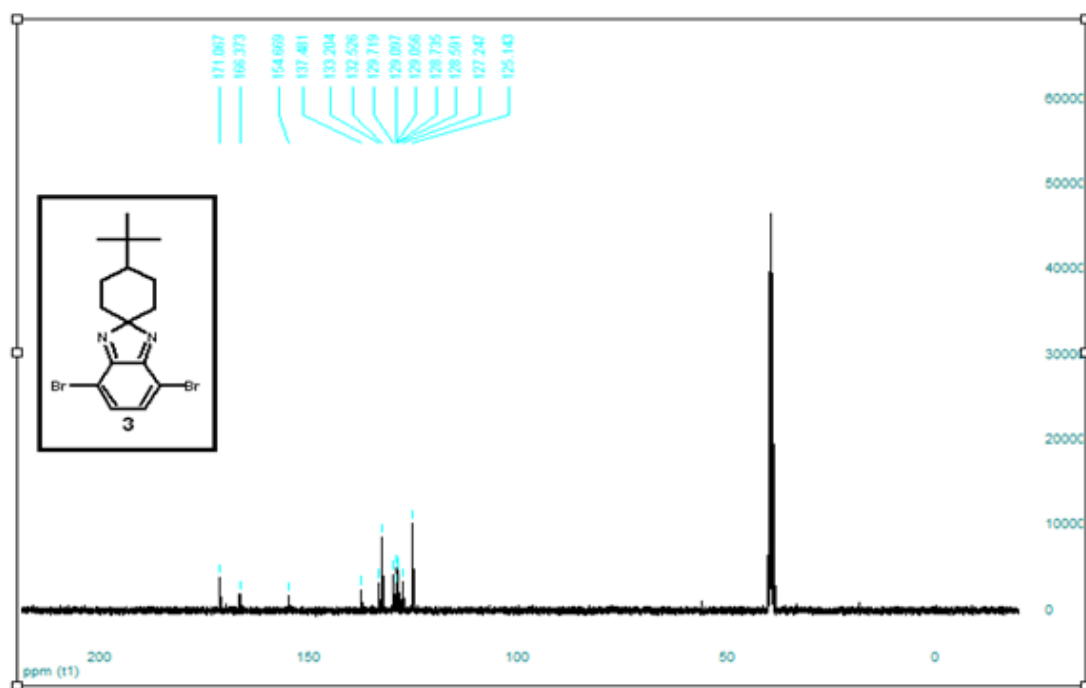


Fig. A. 6. ^{13}C -NMR spectrum of 4, 7-dibromo-4'-(tert-butyl)spiro[benzo[d]imidazole-2,1'-cyclohexane] (3)

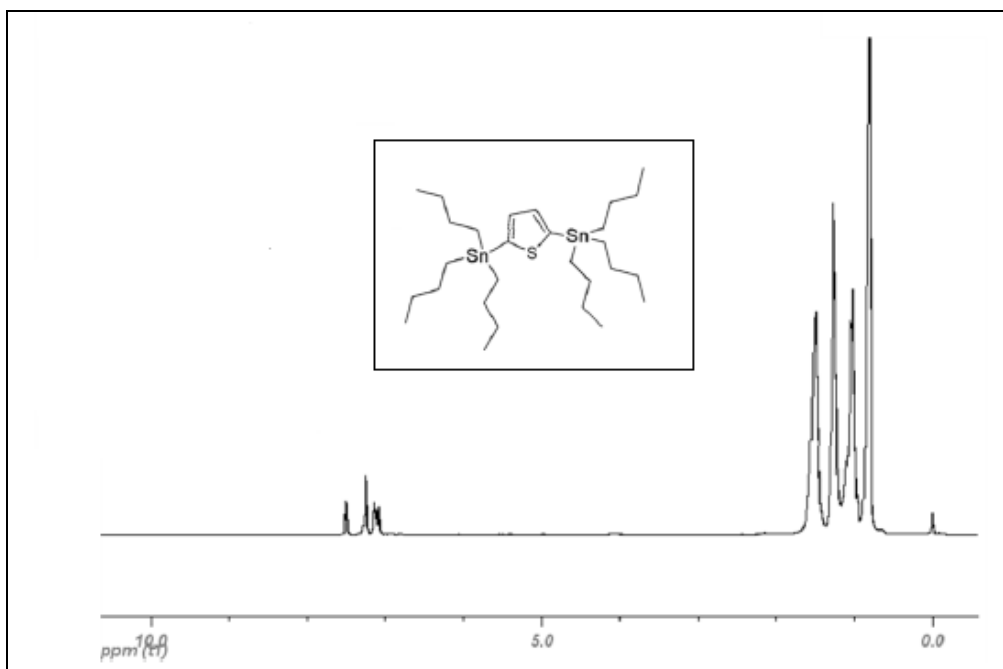


Fig. A.7. ^1H -NMR spectrum of 2,5-bis(tributylstannyl)thiophene

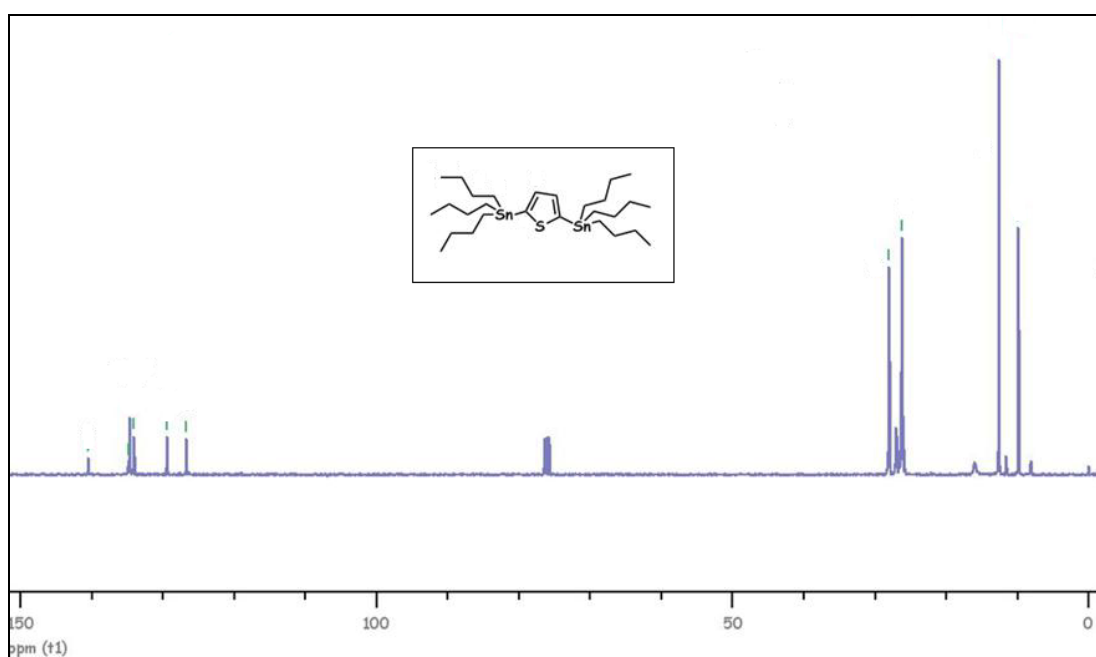


Fig. A. 8. ^{13}C -NMR spectrum of 2,5-bis(tributylstannyl)thiophene

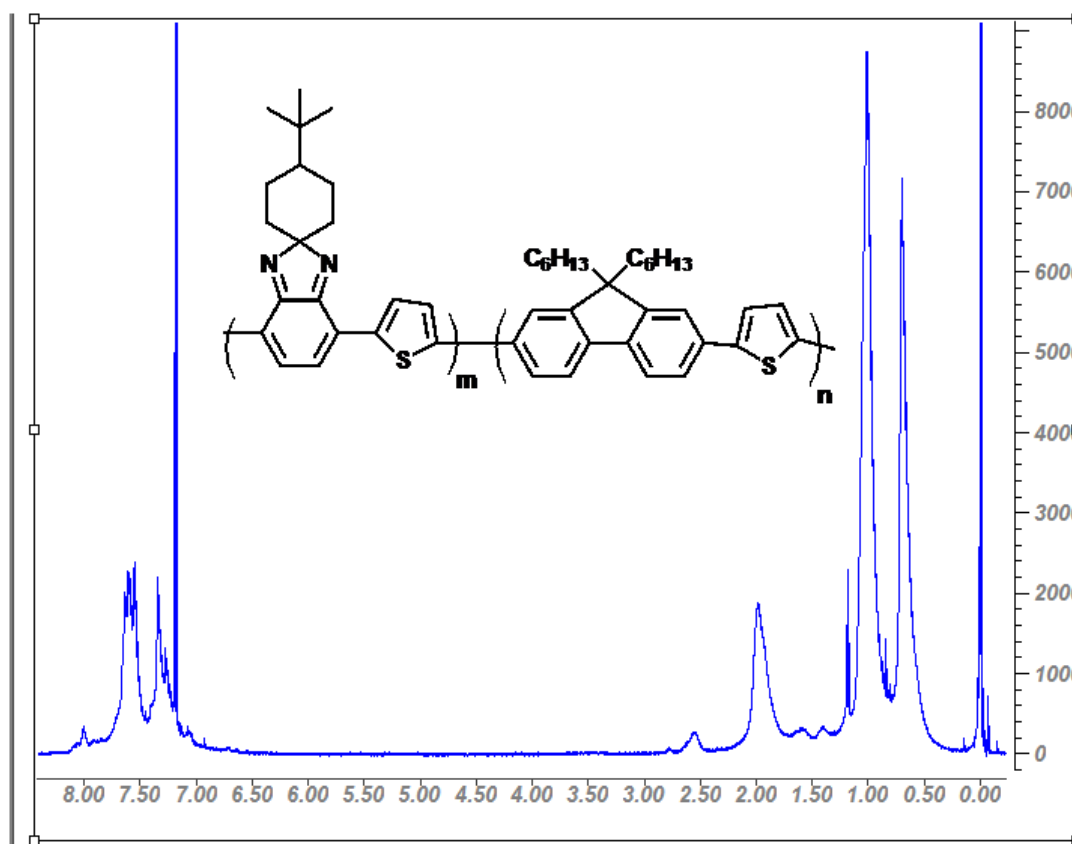


Fig. A. 9. ^1H -NMR spectrum of P1.

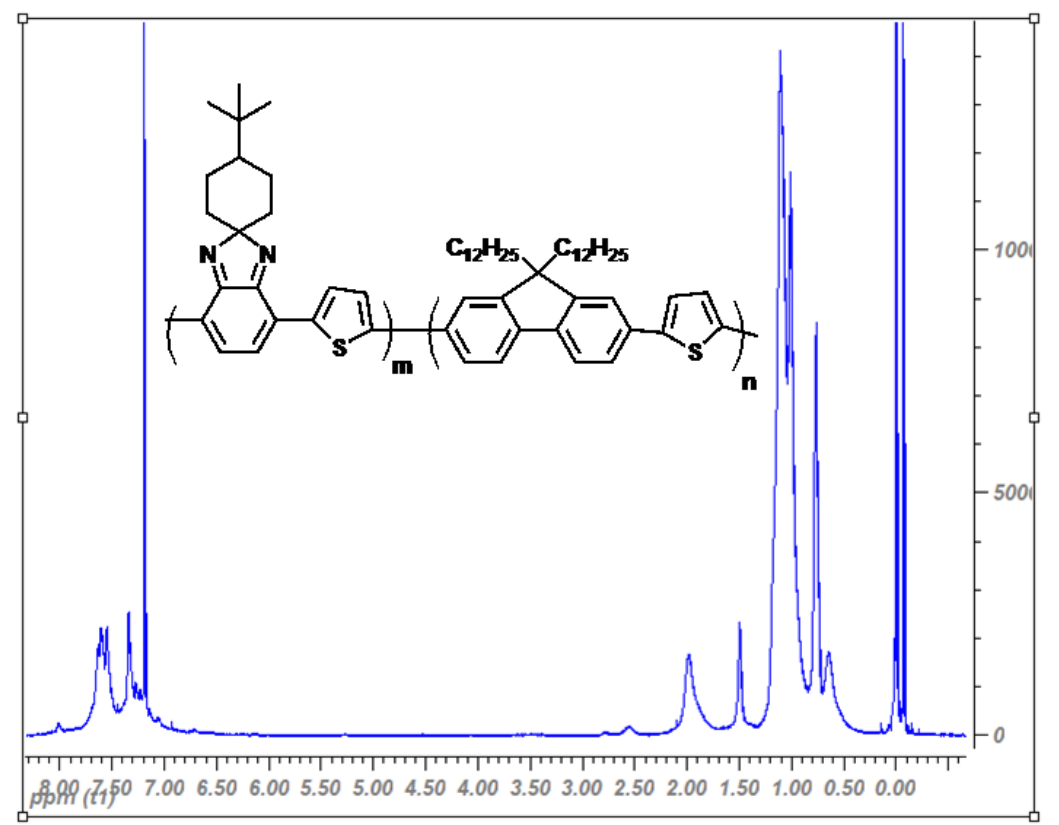


Fig. A. 10. ¹H-NMR spectrum of P2.